ARL-RP-0559 ● Nov 2015


US Army Research Laboratory

# Exact Analytical Solutions for Elastodynamic Impact

by George A Gazonas, Michael J Scheidler, and Ani P Velo

A reprint from International Journal of Solids and Structures, 2015;75–76:172–187.

## NOTICES

### Disclaimers

The findings in this report are not to be construed as an official Department of the Army position unless so designated by other authorized documents.

Citation of manufacturer's or trade names does not constitute an official endorsement or approval of the use thereof.

Destroy this report when it is no longer needed. Do not return it to the originator.

ARL-RP-0559 ● Nov 2015

US Army Research Laboratory

# Exact Analytical Solutions for Elastodynamic Impact

**by George A Gazonas and Michael J Scheidler**
*Weapons and Materials Research Directorate, ARL*

**and**

**Ani P Velo**
*Department of Mathematics and Computer Science, University of San Diego, 5998 Alcalá Park, San Diego, CA 92110*

**A reprint from International Journal of Solids and Structures, 2015;75–76:172–187.**

# REPORT DOCUMENTATION PAGE

*Form Approved*
*OMB No. 0704-0188*



| 1. REPORT DATE *(DD-MM-YYYY)* | 2. REPORT TYPE | 3. DATES COVERED (From - To) |
|---|---|---|
| November 2015 | Reprint | February 2014–August 2015 |

**4. TITLE AND SUBTITLE**
Exact Analytical Solutions for Elastodynamic Impact

**5a. CONTRACT NUMBER**

**5b. GRANT NUMBER**

**5c. PROGRAM ELEMENT NUMBER**

**6. AUTHOR(S)**
George A Gazonas, Michael J Scheidler, and Ani P Velo

**5d. PROJECT NUMBER**
AH-84

**5e. TASK NUMBER**

**5f. WORK UNIT NUMBER**

**7. PERFORMING ORGANIZATION NAME(S) AND ADDRESS(ES)**
US Army Research Laboratory
ATTN: RDRL-WMM-B
Aberdeen Proving Ground, MD 21005-5069

**8. PERFORMING ORGANIZATION REPORT NUMBER**
ARL-RP-0559

**9. SPONSORING/MONITORING AGENCY NAME(S) AND ADDRESS(ES)**

**10. SPONSOR/MONITOR'S ACRONYM(S)**

**11. SPONSOR/MONITOR'S REPORT NUMBER(S)**

**12. DISTRIBUTION/AVAILABILITY STATEMENT**
Approved for public release; distribution is unlimited.

**13. SUPPLEMENTARY NOTES**
A reprint from International Journal of Solids and Structures, 2015;75–76:172–187.

**14. ABSTRACT**

We consider the one-dimensional impact problem in which a semi-infinite flyer collides with (and adheres to) the front face of a stationary target plate of finite thickness, with the back face of the target bonded to another semi-infinite medium. All three bodies are assumed to be linear elastic and homogeneous. Our interest is in explicit expressions for the stress and velocity in the target at all times after impact. The analysis of this problem is simplified by reducing it to an initial-boundary value problem for the target only, which is solved by combining the d'Alembert solution of the wave equation with the Laplace transform method. An appropriate impact boundary condition is required on the front face of the target. In the literature this is usually taken as a prescribed step in stress or velocity, but the correct boundary condition involves a linear combination of the unknown stress and velocity at the impact face. Our solutions are expressed in an apparently new, compact form involving the floor (or greatest-integer) function. The results are amenable to asymptotic analysis; in particular, solutions for stress-free or rigid back faces follow easily as limiting cases of the backing impedance, and the long-time asymptotes of stress and velocity in the target are seen to be independent of the target's elastic properties. All of our results are corroborated by derivation of exact discrete solutions from recursive equations for the impact problems.

**15. SUBJECT TERMS**
One-dimensional impact; Elastic wave propagation; Laplace transform; Floor function; Discrete solutions

| 16. SECURITY CLASSIFICATION OF: | | | 17. LIMITATION OF ABSTRACT | 18. NUMBER OF PAGES | 19a. NAME OF RESPONSIBLE PERSON |
|---|---|---|---|---|---|
| a. REPORT | b. ABSTRACT | c. THIS PAGE | UU | 22 | George A Gazonas |
| Unclassified | Unclassified | Unclassified | | | 19b. TELEPHONE NUMBER (Include area code) 410-306-0863 |

International Journal of Solids and Structures 75–76 (2015) 172–187

Contents lists available at ScienceDirect

International Journal of Solids and Structures

journal homepage: www.elsevier.com/locate/ijsolstr

# Exact analytical solutions for elastodynamic impact

G.A. Gazonas [a,*], M.J. Scheidler [a], A.P. Velo [b]

[a] U.S. Army Research Laboratory, Weapons and Materials Research Directorate, Aberdeen Proving Ground, MD 21005, USA
[b] Department of Mathematics and Computer Science, University of San Diego, 5998 Alcalá Park, San Diego, CA 92110, USA

ARTICLE INFO

*Article history:*
Received 5 March 2015
Received in revised form 14 August 2015
Available online 29 August 2015

*Keywords:*
One-dimensional impact
Elastic wave propagation
Laplace transform
Floor function
Discrete solutions

ABSTRACT

We consider the one-dimensional impact problem in which a semi-infinite flyer collides with (and adheres to) the front face of a stationary target plate of finite thickness, with the back face of the target bonded to another semi-infinite medium. All three bodies are assumed to be linear elastic and homogeneous. Our interest is in explicit expressions for the stress and velocity in the target at all times after impact. The analysis of this problem is simplified by reducing it to an initial-boundary value problem for the target only, which is solved by combining the d'Alembert solution of the wave equation with the Laplace transform method. An appropriate impact boundary condition is required on the front face of the target. In the literature this is usually taken as a prescribed step in stress or velocity, but the correct boundary condition involves a linear combination of the unknown stress and velocity at the impact face. Our solutions are expressed in an apparently new, compact form involving the floor (or greatest-integer) function. The results are amenable to asymptotic analysis; in particular, solutions for stress-free or rigid back faces follow easily as limiting cases of the backing impedance, and the long-time asymptotes of stress and velocity in the target are seen to be independent of the target's elastic properties. All of our results are corroborated by derivation of exact discrete solutions from recursive equations for the impact problems.

Published by Elsevier Ltd.

## 1. Introduction

A large body of the literature concerning analytical or computational solutions to "impact" problems assumes an impact condition in the form of an applied step in velocity or stress on the face of the body being impacted (Ma and Huang, 1996; Lapczyk et al., 1998; Wang and Sun, 2002; Dayal and Bhattacharya, 2006; Wuensche et al., 2009; Sun et al., 2013; Talebian et al., 2013; Dutta et al., 2013). However, for true impact in which at least one of the bodies has finite thickness, is multilayered or is continuously inhomogeneous, multiple reflected or scattered waves will arrive at the impact face and alter the stress and velocity there. Consequently, the history of the stress and the particle velocity at the impact face is generally time-dependent and may be difficult to determine in advance of solution to the problem.

In the current study, we consider the one-dimensional, normal impact problem in which a semi-infinite flyer collides with a stationary target plate of finite thickness $l$, with the rear face of the target bonded to a semi-infinite backing medium (see Fig. 1). The flyer, target and backing medium are assumed to be linear elastic and homogeneous with generally distinct elastic properties. We also assume that the flyer adheres (or "welds") to the front face of the target, in the sense that we do not allow separation of the flyer and target after impact in those cases where wave reflections would otherwise have resulted in separation.[1] Of course, this welding assumption is superfluous in those cases where separation would not have occurred.

We are primarily interested in deriving closed-form expressions for the stress and particle velocity in the target at all times after impact. The solution to this problem is simplified by applying appropriate boundary conditions to both faces of the target, so that the one-dimensional wave equation need only be solved in the target itself. With the $x$-axis oriented as shown in Fig. 1, let $\sigma_1(x,t)$ and $v_1(x,t)$ denote the stress and particle velocity at the point $x$ in the target at time $t$, and let $z_0$ denote the impedance of the flyer. Then the appropriate *impact boundary condition* on the front face of the target ($x = 0$) is

$$z_0 v_1(0,t) \pm \sigma_1(0,t) = z_0 V_0 H(t), \tag{1}$$

* Corresponding author. Tel.: +1 410 306 0863; fax: +1 410 306 0759.
*E-mail address:* george.a.gazonas.civ@mail.mil (G.A. Gazonas).

[1] Such a physical mechanism is known to govern the impact restitution of colliding bodies (Nicholas and Recht, 1990; Shi, 1998; Stronge, 2000; Goldsmith, 2001).

http://dx.doi.org/10.1016/j.ijsolstr.2015.08.011
0020-7683/Published by Elsevier Ltd.

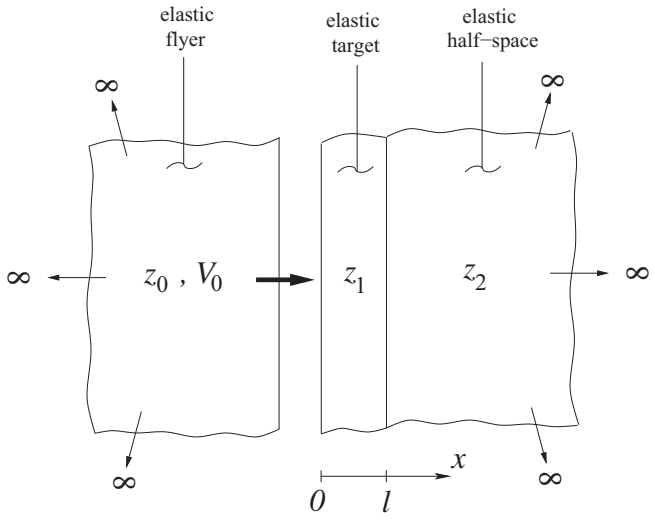


**Fig. 1.** A semi-infinite flyer impacting a target of length $l$ with impact speed $V_0$. The back surface of the target is bonded to a half-space.

where $H$ denotes the Heaviside step function and $V_0$ is speed of the flyer at the moment of impact ($t = 0$). The "+" sign in (1) is used when stress is taken positive in compression and the "−" sign when stress is taken positive in tension. Note that in applying (1), the particle velocity and stress at the impact face, $v_1(0,t)$ and $\sigma_1(0,t)$, are regarded as unknown—it is the relationship between them that determines a boundary condition corresponding to impact. Furthermore, given our assumptions on the flyer, this impact boundary condition is (with some qualifications) independent of the configuration and properties of the target and of the initial conditions within the target (see Section 3.2). Hence, (1) may be applied to other one-dimensional impact problems where interfacial physics effects such as adhesion (Jayadeep et al., 2014) are negligible. Alternatively, for computational code verification purposes (1) is sufficient, but for computational code validation, one may also need to include interface physics effects (Jayadeep et al., 2014; Israelachvili, 1991) in models of impact phenomena.

Condition (1) was used (without proof) by Scheidler and Gazonas (2001) in a study of impact of a semi-infinite flyer on inhomogeneous elastic media; see also Nicholas and Recht (1990, Section 1.3.3) for a different impact problem. Chen et al. (2004) have emphasized the need to account for time dependence of the stress at the impact face for plate impact on periodically layered media; and while their analysis properly accounted for this time dependence, they did not state or use the impact boundary condition (1).

Our paper is organized as follows. Section 2 contains a brief discussion of the d'Alembert solution of the one-dimensional wave equation for a linear elastic solid; this is limited to results that will be used in the sequel. This section also serves to establish notation and sign conventions. Section 3 contains our derivation of the impact boundary condition (1), which utilizes the d'Alembert solution of the wave equation in the flyer. Some alternative forms of this condition are discussed, and we determine when the "impact" boundary conditions commonly used in the literature are correct — either exactly or in some asymptotic sense.

In Section 4 we derive simple, explicit formulas for the stress and velocity in the target for the impact problem described above. We utilize the impact boundary condition (1) on the front face of the target and an appropriate boundary condition on the back face, so that the one-dimensional wave equation need only be solved within the target. We show that the stress and velocity in the target can be obtained from the solution of a difference equation for one of the d'Alembert functions; the Laplace transform method is used to obtain this solution in terms of a series of Heaviside functions. Next, from the Heaviside series we obtain simpler expressions for the two d'Alembert functions in terms of the floor (or greatest-integer) function, and these results are used to derive several simple, explicit formulas for the stress and velocity in the target. These concise relations are valid for all times after impact and all points in the target. In Section 5 we use these results to evaluate the velocity and stress on either side of the shock.

Additional properties of the solutions are discussed in Sections 6 and 7. In Section 6 we determine the long time asymptotes of the velocity and stress in the target and show that they are independent of the properties of the target. We also determine the conditions for which the stress at the impact face of the target can (temporarily) become tensile — a situation that indicates separation of the flyer and target would have occurred were it not for the assumption that they weld on impact. In Section 7 we obtain solutions for the special cases where the back face of the target is either stress-free or rigid. These cases are not included in the main results, which assume that the impedance of the backing medium, $z_2$, is nonzero and finite. However, solutions for the stress-free and rigid cases follow easily from our main results by taking the limits as $z_2 \to 0$ or $\infty$, respectively.

Section 8 contains plots of the stress and velocity histories at either the front face or the midpoint of the target for four different impact problems. For comparison with these analytical solutions, the figures also include the discrete solutions of a recursive system of equations for impact on multi-layered targets, derived elsewhere (Gazonas and Velo, in preparation), and applied to the impact boundary value problem studied here. We close with a discussion of various methods that have been used for solving one-dimensional, linear elastic, impact-type problems and some conclusions regarding the implications of the techniques used here for other elastodynamic problems (Section 9). Closed-form expressions for the jumps in stress and velocity within the target are derived in Appendix A.

## 2. The d'Alembert solution of the wave equation

This section contains a brief discussion of the d'Alembert solution of the one-dimensional wave equation for a linear elastic solid (Graff, 1975; Eringen and Şuhubi, 1975; Achenbach, 1984; Drumheller, 1998; Davison, 2008). Only those results used in the sequel are summarized here. This section also serves to establish notation and sign conventions. The subscript $k$ can take the values 0, 1 or 2 for the flyer, target or backing medium, respectively.

### 2.1. Solution for the displacement

We consider one-dimensional deformations of a homogeneous, linear elastic solid, assuming small displacement gradients. Let $u_k(x,t)$ denote the displacement of material $k$ along the direction of impact at the point $x$ at time $t$, measured relative to the initial configuration at $t = 0$, the moment of impact. Let $v_k(x,t)$ and $\sigma_k(x,t)$ denote the corresponding particle velocity and the stress:

$$v_k(x,t) = \frac{\partial u_k}{\partial t}, \quad \sigma_k(x,t) = \pm E_k \frac{\partial u_k}{\partial x}, \tag{2}$$

where $E_k$ is the elastic modulus and $\partial u_k/\partial x$ is the longitudinal strain. Here and below, the top sign corresponds to the convention that stress is positive in tension, the bottom sign to the convention that stress is positive in compression.

For the normal plate impact problem of interest here, there are no other displacement or strain components. The analysis in this paper can also be applied to the impact of isotropic, linear elastic rods provided that lateral inertia can be neglected (Graff, 1975);

the appropriate elastic modulus in this case is the Young's modulus, usually denoted by $E$. For the uniaxial strain state in normal plate impact, the appropriate elastic modulus is the longitudinal modulus. For isotropic materials this is given by $\lambda + 2\mu$ or, equivalently, by $\kappa + \frac{4}{3}\mu$, where $\lambda, \mu$ and $\kappa$ are the Lamé, shear and bulk moduli. There is no standard notation for the longitudinal modulus, so we have simply used $E$ here.

Momentum balance for material $k$ is given by

$$\pm \frac{\partial \sigma_k}{\partial x} = \rho_k \frac{\partial v_k}{\partial t}, \tag{3}$$

where $\rho_k$ is the density, assumed positive. The relations (2) and (3) yield the one-dimensional wave equation for the displacement:

$$c_k^2 \frac{\partial^2 u_k}{\partial x^2} = \frac{\partial^2 u_k}{\partial t^2}, \quad c_k = \sqrt{\frac{E_k}{\rho_k}}, \tag{4}$$

where $c_k$ is the wave speed. Note that the wave equation for $u_k$ is independent of the sign convention for the stress. d'Alembert's *general solution* of the one-dimensional wave Eq. (4) is

$$u_k(x,t) = f_k(t - x/c_k) + g_k(t + x/c_k), \tag{5}$$

where $f_k$ and $g_k$ are arbitrary, sufficiently smooth functions on some interval of the real numbers $\mathbb{R}$. Any initial or boundary conditions impose restrictions on the functions $f_k$ and $g_k$. The first (second) term on the right in (5) represents a plane longitudinal wave propagating in the positive (negative) $x$-direction, which is to the right (left) with the materials oriented as in Fig. 1.

### 2.2. Solution for the velocity and stress

Let $F_k = f_k'$ and $G_k = g_k'$, where a prime superscript denotes the derivative. Then by (2) and (5), the velocity and stress satisfy

$$v_k(x,t) = F_k(t - x/c_k) + G_k(t + x/c_k), \tag{6}$$

and

$$\sigma_k(x,t) = \pm \frac{E_k}{c_k}[-F_k(t - x/c_k) + G_k(t + x/c_k)]. \tag{7}$$

*Henceforth, we take stress positive in compression*, so that the bottom (minus) sign holds in (2), (3) and (7). Then

$$\sigma_k(x,t) = z_k[F_k(t - x/c_k) - G_k(t + x/c_k)], \tag{8}$$

where $z_k$ is the impedance:

$$z_k = \rho_k c_k = \frac{E_k}{c_k} = \sqrt{\rho_k E_k}. \tag{9}$$

Unless stated otherwise, we assume that $z_k, \rho_k, c_k$ and $E_k$ are positive and finite for each $k = 0, 1, 2$. The only exceptions occur at the end of Section 3.4 where some of the material constants in the flyer ($k = 0$) are allowed to approach zero or infinity, and in Sections 7.1 and 7.2 where some of the material constants in the backing medium ($k = 2$) are allowed to approach zero or infinity. From (6) and (8), we see that

$$\begin{aligned} 2F_k(t - x/c_k) &= v_k(x,t) + \sigma_k(x,t)/z_k, \\ 2G_k(t + x/c_k) &= v_k(x,t) - \sigma_k(x,t)/z_k. \end{aligned} \tag{10}$$

These relations are useful for determining the restrictions imposed on $F_k$ and $G_k$ by initial and boundary conditions. The functions and $(x,t) \mapsto F_k(t - x/c_k)$ and $(x,t) \mapsto G_k(t + x/c_k)$ are the Riemann invariants; they are constant on the characteristic curves $t - x/c_k = \textit{constant}$ and $t + x/c_k = \textit{constant}$, respectively.

### 2.3. Conditions at the shock front

In the remainder of the paper we will not work with the displacement $u_k$ directly. Instead, we will utilize the expressions (6), (8) and (10) for the velocity $v_k$, stress $\sigma_k$, and *d'Alembert functions* $F_k$ and $G_k$ for material $k$. For the impact problem considered here, shock waves will be generated in the target, flyer and backing medium. Thus $u_k$ will be continuous but only piecewise smooth, and $v_k, \sigma_k, F_k$ and $G_k$ will be piecewise continuous and piecewise smooth (in fact, piecewise constant). If a shock front is located at the point $x_s$ in material $k$ at time $t_s$, then $v_k(x_s, t_s)$ and $\sigma_k(x_s, t_s)$ are undefined, at least physically, whereas their one-sided limits (see Appendix A) exist and are unequal, by definition. On the other hand, there is no harm in *assigning* a value to the velocity and stress at the shock front — reasonable choices being one of the one-sided limits or their average.

Our solutions for the stress and velocity in the target will be obtained by first solving for the d'Alembert functions $F_1$ and $G_1$ and then using (6) and (8) to obtain $v_1$ and $\sigma_1$. In solving for the piecewise continuous functions $F_1$ and $G_1$, it is mathematically convenient to regard these functions as being defined at all points on some interval of $\mathbb{R}$, their values at any jump discontinuities being given by one of the one-sided limits. Consequently, our solutions for $v_1(x,t)$ and $\sigma_1(x,t)$ will have values assigned on the shock front. These values have no physical significance, and the use of different conventions in assigning values to $F_1$ and $G_1$ at their points of discontinuity could result in different values for $v_1$ and $\sigma_1$ on the shock front.

## 3. The impact boundary condition for a semi-infinite flyer

We begin with the derivation of the boundary condition on the face of the flyer, using the d'Alembert solution of the wave equation in the flyer. This result may also be derived by the method of characteristics. The corresponding impact boundary condition on the target is obtained in Section 3.2. An alternative form of this impact boundary condition is discussed in Section 3.3. In Section 3.4 we determine when the "impact" boundary conditions commonly used in the literature are correct — either exactly or in some asymptotic sense.

### 3.1. Boundary condition on the flyer

Consider a semi-infinite flyer which is initially stress-free and traveling in the positive $x$ direction at uniform speed $V_0$ (see Fig. 1). The flyer impacts the target at the instant $t = 0$; the target and the half-space backing it occupy the region $x \geqslant 0$, and the flyer occupies the half-space $x \leqslant 0$. The initial conditions in the flyer are

$$v_0(x,0) = V_0 > 0 \quad \text{and} \quad \sigma_0(x,0) = 0, \quad x \leqslant 0. \tag{11}$$

The d'Alembert solution for the velocity and stress in the flyer is given by (6) and (8) with $k = 0$. On setting $k = 0$ in $(10)_1$, we have

$$v_0(x,t) + \sigma_0(x,t)/z_0 = 2F_0(t - x/c_0), \quad x \leqslant 0, \ t \geqslant 0. \tag{12}$$

On setting $t = 0$ in (12) and using the initial conditions (11), we see that $V_0 = 2F_0(-x/c_0)$ for $x \leqslant 0$; equivalently, $2F_0(\tilde{t}) = V_0$ for $\tilde{t} \geqslant 0$. Since $t - x/c_0 \geqslant 0$ for $x$ and $t$ as in (12), it follows that

$$v_0(x,t) + \sigma_0(x,t)/z_0 = V_0, \quad x \leqslant 0, \ t \geqslant 0. \tag{13}$$

On setting $x = 0$ in the above, we see that the stress and velocity at the impact face of the flyer are related by

$$z_0 v_0(0,t) + \sigma_0(0,t) = z_0 V_0, \quad t \geqslant 0. \tag{14}$$

### 3.2. Impact boundary condition on the target

Up to this point the target has not entered the analysis. As long as the flyer and target are in contact, their displacements, velocities and stresses must be continuous across the impact interface and hence coincide at the interface. Thus[2]

$$v_1(0,t) = v_0(0,t), \sigma_1(0,t) = \sigma_0(0,t), \quad 0 < t \leqslant t_c, \tag{15}$$

where a "1" subscript is used for target variables and $t_c$ is the duration of contact of the flyer and target, which may be finite or infinite. We do not assume that the velocities of the flyer and target coincide at $t = 0$. Indeed, $v_0(0,0) = V_0$ by (11), whereas the target is assumed to be initially at rest and stress-free:

$$v_1(x,0) = 0, \quad \sigma_1(x,0) = 0, \quad 0 \leqslant x \leqslant l, \tag{16}$$

where $l$ is the length of the target; in particular, $v_1(0,0) = 0$. Thus $v_1(0,0) \neq v_0(0,0)$, and more significantly, $\lim_{x\downarrow 0} v_1(x,0) \neq \lim_{x\uparrow 0} v_0(x,0)$.

The contact relations (15), together with the boundary condition (14) on the flyer, yield a relation between the stress and particle velocity in the target at the impact face $x = 0$:

$$z_0 v_1(0,t) + \sigma_1(0,t) = z_0 V_0, \quad 0 < t \leqslant t_c; \tag{17}$$

see also Nicholas and Recht (1990, Eq. (52)) for impact of a finite flyer on a finite target (with no backing). Our derivation of (17) made essential use of the one-dimensional nature of the impact problem considered here and also of the assumptions that the flyer is homogeneous,[3] linear elastic and semi-infinite. Since no information about the target was utilized in the derivation of (17), it follows that *this impact boundary condition is essentially independent of the configuration and properties of the target and of the initial conditions within the target*.[4] The target need not have elastic (let alone linear elastic) response, it may have any combination of discrete or continuously varying inhomogeneities, and it may be initially deformed and undergoing non-uniform motion.

If the duration of contact is finite, then the front face of the target is unstressed once separation occurs, and the appropriate boundary condition on the front face of the target would be $\sigma_1(0,t) = 0$ for $t_c < t < t_r$, where $t_r$ is the first instant at which the flyer and target regain contact. However, the duration of contact $t_c$ cannot be determined in advance except for the simplest problems. These complications are bypassed by assuming (as is done here) that the flyer and target weld on impact. Then $t_c = \infty$, and the impact boundary condition (17) becomes[5]

$$z_0 v_1(0,t) + \sigma_1(0,t) = z_0 V_0, \quad t > 0. \tag{18}$$

### 3.3. Alternative forms of the impact boundary condition

We begin by considering a minor variation of the impact boundary condition (18) — we assume that it also holds at the moment of impact, $t = 0$:

$$z_0 v_1(0,t) + \sigma_1(0,t) = z_0 V_0, \quad t \geqslant 0. \tag{19}$$

Since this implies $z_0 v_1(0,0) + \sigma_1(0,0) = z_0 V_0$, the initial conditions (16) cannot hold at $x = 0$. Instead, the initial conditions are

$$v_1(x,0) = 0, \quad \sigma_1(x,0) = 0, \quad 0 < x \leqslant l, \tag{20}$$

with $v_1(0,0)$ and $\sigma_1(0,0)$ to be determined, consistent with (19). The impact and initial conditions (19) and (20) differ from (18) and (16) only at a single point in $(x,t)$ space, namely $(x,t) = (0,0)$. One would not expect this difference to appreciably affect the solution. Indeed, the solutions obtained from the two sets of impact and initial conditions differ only in the values assigned to the stress and velocity on the shock front; cf. the discussion in Section 2.3.

We are interested in determining the stress and velocity in the target for all times $t > 0$. Conditions in the target at times $t < 0$ are irrelevant. Nevertheless, if we regard $v_1(x,t)$ and $\sigma_1(x,t)$ as defined for all times $t \in \mathbb{R}$, then we are free to assume that the target was stress-free and at rest for all times prior to impact, so that

$$v_1(x,t) = 0, \quad \sigma_1(x,t) = 0, \quad 0 \leqslant x \leqslant l, \ t < 0. \tag{21}$$

Clearly, the boundary condition (19) would not apply for $t < 0$. On the other hand, if $H$ denotes the Heaviside step function:

$$H(t) = \begin{cases} 0, & t < 0, \\ 1, & t \geqslant 0, \end{cases} \tag{22}$$

then the boundary condition

$$z_0 v_1(0,t) + \sigma_1(0,t) = z_0 V_0 H(t), \quad t \in \mathbb{R} \tag{23}$$

is consistent with both the impact condition (19) and with (21). This is the form in which the impact boundary condition was stated by Scheidler and Gazonas (2001). *The conventions described in this subsection and, in particular, the impact boundary condition in the form (23), will be used in the sequel.*

Finally, recall that the derivation of this impact boundary condition makes essential use of the assumptions that the flyer is homogeneous, linear elastic, and semi-infinite and that the flyer adheres to the target. Note that since the flyer is assumed to have positive density, it necessarily has infinite mass. Consequently, our impact boundary condition is not appropriate for the case of a flyer of finite length and mass.

### 3.4. Common "impact-type" boundary conditions

The two most common "impact-type" boundary conditions used in the literature are a *step in velocity* and a *step in stress:*

$$v_1(0,t) = V_1 H(t), \quad V_1 > 0, \quad t \in \mathbb{R}; \tag{24}$$

and

$$\sigma_1(0,t) = \Sigma_1 H(t), \quad \Sigma_1 > 0, \quad t \in \mathbb{R}. \tag{25}$$

Here $V_1$ and $\Sigma_1$ are assigned constants. In this section we examine when these conditions truly describe impact — either exactly or in some limiting sense.

First, consider the case where *both the flyer and the target are homogeneous, linear elastic and semi-infinite*. Then both (24) and (25) hold with $V_1$ and $\Sigma_1$ determined by the impact speed $V_0$ of the flyer and the impedances $z_0$ and $z_1$ of the flyer and target:

$$V_1 = \frac{z_0}{z_0 + z_1} V_0, \quad \Sigma_1 = z_1 V_1 = \frac{z_0 z_1}{z_0 + z_1} V_0; \tag{26}$$

see Davison (2008, Eq. (3.21)) and the discussion below. Note that $V_1 < V_0$. It is easily verified that the relations (24)–(26) are consistent with the impact boundary condition (23); that is, if (24)–(26) hold then so does (23). Of course, when the assumptions in italics above are satisfied, only one set of conditions, either (24) and

[2] These relations do not strictly hold at an instant $t = t_s$ at which the shock front (reflected from the back surface of the target) arrives at the flyer/target interface, since the velocity and stress are undefined at this instant. However, (15) holds in the sense that $v_1(0,t)$ and $v_0(0,t)$ have the same the one-sided limits as $t \to t_s$ from above or below, and similarly for the stresses.

[3] It can be shown (by a different method) that (17) continues to hold if the density, elastic modulus and wave speed of the flyer vary with position in such a way that the impedance of the flyer is constant.

[4] This statement requires some qualifications. The duration of contact $t_c$ clearly depends on both the configuration and properties of the target. The initial velocity of the target (if any) at $x = 0$ must be less than $V_0$ in order for impact to occur. Any variations in target properties or initial conditions must be in the $x$-direction only, so that the one-dimensional nature of the problem is retained and, in particular, so that the stress and particle velocity on the impact face are uniform.

[5] If stress had been taken positive in tension, then the appropriate boundary condition would be $z_0 v_1(0,t) - \sigma_1(0,t) = z_0 V_0$.

$(26)_1$ or (25) and $(26)_2$, would have to be imposed as a boundary condition on the target. From (26) it follows that

$$\begin{aligned} V_0 &= \tfrac{z_0+z_1}{z_0} V_1 = \tfrac{z_0+z_1}{z_0 z_1} \Sigma_1, \\ z_0 &= \tfrac{V_1}{V_0-V_1} z_1 = \tfrac{\Sigma_1}{z_1 V_0 - \Sigma_1} z_1. \end{aligned} \tag{27}$$

Thus for a given flyer impedance $z_0$, the boundary condition (24) holds for an arbitrarily prescribed $V_1$ provided that the impact speed of the flyer is given by the first expression for $V_0$ in (27); and the boundary condition (25) holds for an arbitrarily prescribed $\Sigma_1$ provided that the impact speed of the flyer is given by the second expression for $V_0$ in (27). Similarly, for a given flyer speed $V_0$, the boundary condition (24) holds for an arbitrarily prescribed $V_1 < V_0$ provided that the impedance of the flyer is given by the first expression for $z_0$ in (27); and the boundary condition (25) holds for an arbitrarily prescribed $\Sigma_1 < z_1 V_0$ provided that the impedance of the flyer is given by the second expression for $z_0$ in (27).

The boundary condition (24) or (25) is often used for "impact-type" problems in which the conditions in italics above are not satisfied. While there is nothing inherently wrong with this, neither (24) nor (25) is the appropriate boundary condition for *impact* in such cases. For example, consider a homogeneous, linear elastic target of finite length $l$, with or without a backing medium. Let $t_*$ denote the travel time in the target, that is, the time it takes the shock wave to travel the length of the target:

$$t_* = \frac{l}{c_1}. \tag{28}$$

Then $2t_*$ is the time it takes the shock wave to travel from the front (impact) face of the target, reflect off the back face, and return to the front face. If (24)–(26) are indeed valid for a semi-infinite target, then one would expect that these relations hold for all times $t < 2t_*$ in the finite target, but generally not beyond that. In Section 5.3 we will show that this result follows easily from our explicit solutions. For a semi-infinite target, the relations (24)–(26) follow by taking the limit of the result for the finite target as its length $l$, and hence the travel time $t_*$, approaches infinity.

Finally, we indicate how *the "impact-type" boundary conditions (24) and (25) can be obtained as (different) extreme limiting cases of the true impact boundary condition (23), without imposing any conditions on the target*. First, let $V_0 = V_1$ and write (23) as $v_1(0,t) = V_1 H(t) - \sigma_1(0,t)/z_0$. Then (24) holds in the limit as the impedance $z_0$ of the flyer becomes infinite. By (9) with $k = 0$, this latter condition corresponds to a flyer of infinite modulus and non-zero density (i.e., a rigid flyer), or a flyer of infinite density and non-zero modulus. Next, let $V_0 = \Sigma_1/z_0$, in which case (23) can be written as $\sigma_1(0,t) = \Sigma_1 H(t) - z_0 v_1(0,t)$. Then we obtain (25) in the limit as the impedance of the flyer goes to zero with $\Sigma_1$ fixed, in which case the speed of the flyer becomes infinite. By Eq. (9), the flyer has zero impedance if the density is zero and the elastic modulus is positive and finite, or vice versa.

## 4. Solution in the target by combined d'Alembert and Laplace transform methods

In this section we derive explicit formulas for the stress and velocity in the target for the impact problem described in the introduction. We utilize the impact boundary condition on the front face of the target (Section 3) and an appropriate boundary condition on the back face (Section 4.1). In Section 4.2 we express the impact problem in non-dimensional form and show that the non-dimensional stress and velocity in the target can be obtained from the solution of a difference equation for one of the non-dimensional d'Alembert functions. In Section 4.3 we use the Laplace transform method to obtain the solution of this difference equation in terms of a series of Heaviside functions. A simpler form of the solution for the two non-dimensional d'Alembert functions in terms of the floor (or greatest-integer) function is obtained in Section 4.4, and these results are used in Section 4.5 to obtain several simple, explicit formulas for the non-dimensional stress and velocity in the target. These results are recast in dimensional form in Section 4.6. We follow the conventions in Section 3.3; in particular, we regard the stress and velocity as defined for all times $t \in \mathbb{R}$. However, the explicit formulas for the stress and velocity in Section 4.6 are only valid for $t \geqslant 0$.

### 4.1. Back face boundary condition

The d'Alembert solution for the velocity and stress in the half-space backing the target are given by (6) and (8) with $k = 2$. On setting $k = 2$ in $(10)_2$, we have

$$2G_2(t + x/c_2) = v_2(x,t) - \sigma_2(x,t)/z_2, \quad t \in \mathbb{R},\ x \geqslant l. \tag{29}$$

The domain of $G_2$ is all of $\mathbb{R}$. Since the half-space is at rest and unstressed for all times $t \leqslant 0$, the right-hand side of (29) is zero for $t \leqslant 0$ and $x \geqslant l$. As $x$ and $t$ range over these semi-infinite intervals, $t + x/c_2$ takes on all real values. Hence $G_2 \equiv 0$, and (29) reduces to

$$\sigma_2(x,t) = z_2 v_2(x,t), \quad t \in \mathbb{R},\ x \geqslant l. \tag{30}$$

In particular, at the interface with the target ($x = l$), the velocity and stress in the half-space are related by

$$\sigma_2(l,t) = z_2 v_2(l,t), \quad t \in \mathbb{R}. \tag{31}$$

Then by continuity of stress and velocity across material interfaces, the velocity and stress in the target at $x = l$ are related by[6]

$$\sigma_1(l,t) = z_2 v_1(l,t), \quad t \in \mathbb{R}. \tag{32}$$

This boundary condition, like the impact boundary condition (18), is independent of the properties of the target.

### 4.2. The d'Alembert solution in the target

From the d'Alembert solution of the wave equation, the velocity and stress in the target are given by (6) and (8) with $k = 1$:

$$\begin{aligned} v_1(x,t) &= F_1(t - x/c_1) + G_1(t + x/c_1), \\ \sigma_1(x,t) &= z_1[F_1(t - x/c_1) - G_1(t + x/c_1)]. \end{aligned} \tag{33}$$

for $t \in \mathbb{R}$ and $0 \leqslant x \leqslant l$. The domains of $F_1$ and $G_1$ are all of $\mathbb{R}$. Recall that the initial conditions are given by (20) and the conditions prior to impact by (21). On setting $k = 1$ in (10) and using (20) and (21), we obtain the following restrictions on the d'Alembert functions $F_1$ and $G_1$:

$$F_1(\tilde{t}) = 0,\ \tilde{t} < 0 \quad \text{and} \quad G_1(\tilde{t}) = 0,\ \tilde{t} \leqslant t_* = l/c_1. \tag{34}$$

The derivation of the solutions for $F_1$ and $G_1$, and the subsequent expressions for $v_1(x,t)$ and $\sigma_1(x,t)$, are simplified if we cast the problem in non-dimensional form. We define the non-dimensional distance $y$ and time $\tau$ by

$$y \equiv \frac{x}{l} = \frac{x}{c_1 t_*}, \quad \tau \equiv \frac{t}{t_*} = \frac{c_1 t}{l}; \tag{35}$$

then $0 \leqslant y \leqslant 1$ and $\tau \in \mathbb{R}$. For $t > 0$, $c_1 t$ is the total distance (including reflections) that the wave has traveled from the moment of impact; hence $\tau$ is also the total non-dimensional distance the wave has traveled from the moment of impact. The velocity and stress are often non-dimensionalized by dividing by the wave speed and elas-

[6] If stress had been taken positive in tension, then the appropriate boundary condition would be $\sigma_1(l,t) + z_2 v_1(l,t) = 0$; see also Nonaka et al. (1996, Eq. (17)).

tic modulus, respectively. For the impact problem considered here, it turns out to be more convenient to use

$$v(y,\tau) \equiv \frac{v_1(x,t)}{V_1}, \quad \sigma(y,\tau) \equiv \frac{\sigma_1(x,t)}{\Sigma_1} \tag{36}$$

for the non-dimensional velocity and stress. Recall that $V_1$ and $\Sigma_1$ are given in terms of the impact speed $V_0$ and the impedances $z_0$ and $z_1$ of the flyer and target by the expressions in (26). This choice is motivated by the fact that $V_1$ and $\Sigma_1$ are the initial jumps in velocity and stress in the target (see Section 5); however, at this point we simply regard the expressions in (26) as definitions of $V_1$ and $\Sigma_1$.

On dividing the impact boundary condition (23) by $z_0V_0$ and then using (35), (36) with $x = 0$, the expressions (26) for $V_1$ and $\Sigma_1$, and the fact that $H(t) = H(\tau)$, we obtain

$$\frac{z_0}{z_0+z_1}\, v(0,\tau) + \frac{z_1}{z_0+z_1}\, \sigma(0,\tau) = H(\tau), \quad \tau \in \mathbb{R}. \tag{37}$$

Similarly, on dividing the back face boundary condition (32) by $\Sigma_1$ and using (26), (35) and (36) with $x = l$, we obtain

$$\sigma(1,\tau) = \frac{z_2}{z_1}\, v(1,\tau), \quad \tau \in \mathbb{R}. \tag{38}$$

These are the non-dimensional forms of the boundary conditions on the target. Since the d'Alembert functions $F_1$ and $G_1$ have the dimensions of velocity and since, by (35),

$$t \pm x/c_1 = t_*(\tau \pm y), \tag{39}$$

we define non-dimensional d'Alembert functions $F$ and $G$ as follows:

$$F(\tau) \equiv \frac{F_1(t_*\tau)}{V_1}, \quad G(\tau) \equiv \frac{G_1(t_*\tau)}{V_1}. \tag{40}$$

Then by (33), (36), (39) and (40), the d'Alembert solution for the non-dimensional velocity and stress in the target is

$$\begin{aligned} v(y,\tau) &= F(\tau - y) + G(\tau + y), \\ \sigma(y,\tau) &= F(\tau - y) - G(\tau + y), \end{aligned} \tag{41}$$

for $\tau \in \mathbb{R}$ and $0 \leqslant y \leqslant 1$. The domains of $F$ and $G$ are all of $\mathbb{R}$.

The following non-dimensional parameters occur repeatedly in the sequel:

$$a = \frac{z_0 - z_1}{z_0 + z_1}, \quad b = \frac{z_2 - z_1}{z_2 + z_1}, \quad A = ab. \tag{42}$$

Since the impedances are positive,

$$|a| < 1, \quad |b| < 1, \quad |A| < 1. \tag{43}$$

On substituting (41) with $y = 0$ into the non-dimensional impact boundary condition (37) and rearranging terms, we obtain

$$F(\tau) + aG(\tau) = H(\tau), \quad \tau \in \mathbb{R}. \tag{44}$$

Similarly, on substituting (41) with $y = 1$ into the non-dimensional back face boundary condition (38) and rearranging terms, we obtain

$$G(\tau + 1) = -bF(\tau - 1), \quad \tau \in \mathbb{R}. \tag{45}$$

Also, by (40), the non-dimensional form of the initial conditions (34) is

$$F(\tau) = 0, \ \tau < 0 \quad \text{and} \quad G(\tau) = 0, \ \tau \leqslant 1. \tag{46}$$

Next, observe that the relation (45) is equivalent to

$$G(\tau) = -bF(\tau - 2), \quad \tau \in \mathbb{R}. \tag{47}$$

On substituting this relation into (44) and using $(42)_3$, we obtain the following difference equation for $F$:

$$F(\tau) - AF(\tau - 2) = H(\tau), \quad \tau \in \mathbb{R}. \tag{48}$$

Also note that by (47) and $(46)_1$, the condition $(46)_2$ can be strengthened to

$$G(\tau) = 0, \quad \tau < 2. \tag{49}$$

In the next section, we will see that the difference Eq. (48) for $F$, subject to the initial condition $(46)_1$, is easily solved by the Laplace transform method. Then the solution for $G$ follows from (47), and the non-dimensional velocity and stress can be obtained from (41).

### 4.3. Solution for F by Laplace transforms

Let $f$ denote a real-valued, piecewise-continuous function defined on $\mathbb{R}$, with

$$f(\tau) = 0, \quad \tau < 0. \tag{50}$$

We employ the right-sided or unilateral Laplace transform of $f$ (Doetsch, 1974):

$$\bar{f}(s) = \mathcal{L}\{f\}(s) = \mathcal{L}_\tau\{f(\tau)\}(s) \equiv \int_0^\infty f(\tau)\, e^{-s\tau} d\tau, \tag{51}$$

where $s = \sigma + i\omega$ is generally a complex number with $\Re(s) > 0$. The Laplace transform of the Heaviside step function is given by

$$\bar{H}(s) = \frac{1}{s}. \tag{52}$$

We also need the Laplace shifting theorem for functions satisfying (50): if $\tau_1 > 0$, then

$$\mathcal{L}_\tau\{f(\tau - \tau_1)\}(s) = e^{-s\tau_1}\bar{f}(s). \tag{53}$$

On taking the Laplace transform of the difference Eq. (48) for $F$ and using (52), $(46)_1$, and (53) with $f = F$ and $\tau_1 = 2$, we obtain

$$(1 - Ae^{-2s})\bar{F}(s) = \frac{1}{s}. \tag{54}$$

Since $\Re(s) > 0$, we have $|e^{-2s}| = e^{-2\Re(s)} < 1$, so that by $(43)_3$, $|Ae^{-2s}| < |A| < 1$. Hence $1 - Ae^{-2s} \neq 0$, and (54) yields the following expressions for the Laplace transform of $F$:

$$\bar{F}(s) = \frac{1}{s}\frac{1}{1 - Ae^{-2s}} = \frac{1}{s}\left[1 + \sum_{n=1}^{\infty}(Ae^{-2s})^n\right] = \frac{1}{s} + \sum_{n=1}^{\infty} A^n \frac{1}{s}\, e^{-2ns}. \tag{55}$$

The inverse transform of (55) yields the non-dimensional d'Alembert function $F$. On using (52) and the shifting theorem (53) with $f = H$ and $\tau_1 = 2n$, we see that

$$\frac{1}{s}\, e^{-2ns} = \mathcal{L}_\tau\{H(\tau - 2n)\}(s). \tag{56}$$

Then by (56) and (52) it follows that $F$ is given by

$$F(\tau) = H(\tau) + \sum_{n=1}^{\infty} A^n H(\tau - 2n), \quad \tau \in \mathbb{R}; \tag{57}$$

and by (47),

$$G(\tau) = -bH(\tau - 2) - b\sum_{n=1}^{\infty} A^n H(\tau - 2(n+1)), \quad \tau \in \mathbb{R}. \tag{58}$$

It follows that $F$ has jump discontinuities at the non-dimensional times $\tau = 0, 2, 4, \ldots$; and $G$ has jump discontinuities at the non-dimensional times $\tau = 2, 4, 6, \ldots$

If $\tau < 0$, then $H(\tau) = H(\tau - 2n) = 0$, and we recover the initial condition $(46)_1$ from (57). More generally, for any $\tau \in \mathbb{R}$ there are only a finite number (possibly zero) of nonzero terms in the sum in (57), since

$$H(\tau - 2n) = 0 \quad \text{iff} \quad \tau - 2n < 0 \quad \text{iff} \quad n > \tau/2; \tag{59}$$

and $H(\tau - 2n) = 1$ otherwise, that is for $n \leqslant \tau/2$. Thus (57) reduces to

$$F(\tau) = H(\tau) + \sum_{1 \leqslant n \leqslant \tau/2} A^n, \quad \tau \in \mathbb{R}, \tag{60}$$

provided the sum is regarded as zero if there is no integer $n$ satisfying $1 \leqslant n \leqslant \tau/2$, that is, if $\tau/2 < 1$. An analogous result holds for $G$.

### 4.4. Solution for F and G in terms of the floor function

If $\tau$ is not a positive even integer, then there will be no integer $n \geqslant 1$ that is equal to $\tau/2$, in which case it would not be correct to write the sum in (60) as $\sum_{n=1}^{\tau/2} A^n$. Let $\mathbb{Z}$ denote the set of integers. The floor function (or greatest-integer function) $\lfloor\cdot\rfloor : \mathbb{R} \to \mathbb{Z}$ is defined by the condition that $\lfloor r \rfloor$ is the greatest integer less than or equal to the real number $r$. Some properties of the floor function are listed below; here $r$ is a real number and $n$ and $m$ are integers:

$$n \leqslant r < n+1 \iff \lfloor r \rfloor = n, \quad \lfloor r \pm n \rfloor = \lfloor r \rfloor \pm n, \tag{61}$$

$$n \leqslant r \iff n \leqslant \lfloor r \rfloor, \quad r < m \iff \lfloor r \rfloor \leqslant m-1. \tag{62}$$

On setting $r = \tau/2$ in the left relation in (62), we see that (60) can be written as[7]

$$F(\tau) = H(\tau) + \sum_{n=1}^{\lfloor \tau/2 \rfloor} A^n, \quad \tau \in \mathbb{R}, \tag{63}$$

provided the sum is regarded as zero if $\lfloor \tau/2 \rfloor < 1$, equivalently, if $\tau < 2$. In particular, (63) yields

$$F(\tau) = \begin{cases} 0, & \tau < 0, \\ 1, & 0 \leqslant \tau < 2, \\ 1 + A, & 2 \leqslant \tau < 4. \end{cases} \tag{64}$$

Next, we claim that

$$F(\tau) = \frac{1 - A^{\lfloor \tau/2 \rfloor + 1}}{1 - A}, \quad \tau \geqslant -2, \tag{65}$$

provided that we use the convention $0^0 \equiv 1$ when $A = 0$. Since $A^0 = 1$ for any nonzero $A$, this convention implies

$$A^0 = 1. \tag{66}$$

for all $A$. To prove the claim, first note that for any real number $q \neq 1$ and any integer $N \geqslant 1$,

$$1 + \sum_{n=1}^{N} q^n = \frac{1 - q^{N+1}}{1 - q}. \tag{67}$$

This relation also holds for $N = 0$ provided the sum is regarded as zero in this case. Suppose that $\tau \geqslant 0$. Then by (63), $F(\tau) = 1 + \sum_{n=1}^{\lfloor \tau/2 \rfloor} A^n$. Since $A \neq 1$ and since $\lfloor \tau/2 \rfloor \geqslant 0$ in this case, we may apply (67) with $q = A$ and $N = \lfloor \tau/2 \rfloor$, which yields the expression in (65). Now suppose that $-2 \leqslant \tau < 0$. In this case $\lfloor \tau/2 \rfloor = -1$, so the right-hand side of (65) reduces to $(1 - A^0)/(1 - A)$, which is zero by the convention (66). Since $F(\tau) = 0$ for $\tau < 0$, (65) gives the correct result for $-2 \leqslant \tau < 0$, which proves the claim.The concise expression in (65) is not valid for $\tau < -2$ since it yields a nonzero result. However, a closed-form expression for $F(\tau)$ for $\tau \geqslant -2$ is all that is really needed here, since by (47) it yields a closed-form expression for $G(\tau)$ for $\tau \geqslant 0$. Indeed, since $\lfloor (\tau - 2)/2 \rfloor = \lfloor \tau/2 - 1 \rfloor = \lfloor \tau/2 \rfloor - 1$, from (47) and (65) we obtain

$$G(\tau) = -b \frac{1 - A^{\lfloor \tau/2 \rfloor}}{1 - A}, \quad \tau \geqslant 0. \tag{68}$$

The concise expression in (68) is not valid for $\tau < 0$ since it yields a nonzero result, contrary to (49). However, for $0 \leqslant \tau < 2$ we have $\lfloor \tau/2 \rfloor = 0$ and thus $A^{\lfloor \tau/2 \rfloor} = 1$, so that $G(\tau) = 0$, consistent with (49). For $2 \leqslant \tau < 4$ we have $\lfloor \tau/2 \rfloor = 1$, so that (68) yields

$$G(\tau) = -b, \quad 2 \leqslant \tau < 4. \tag{69}$$

### 4.5. Expressions for the non-dimensional velocity and stress in the target

On substituting the expressions (65) and (68) for $F$ and $G$ into the relations (41) for the non-dimensional velocity and stress, we obtain the compact formulas

$$v(y,\tau) = \frac{1}{1-A}\left[1 - A^{\lfloor (\tau - y)/2 \rfloor + 1} - b\left(1 - A^{\lfloor (\tau + y)/2 \rfloor}\right)\right], \tag{70}$$

$$\sigma(y,\tau) = \frac{1}{1-A}\left[1 - A^{\lfloor (\tau - y)/2 \rfloor + 1} + b\left(1 - A^{\lfloor (\tau + y)/2 \rfloor}\right)\right]. \tag{71}$$

These relations and those below are valid for all $0 \leqslant y \leqslant 1$ but only for $\tau \geqslant 0$. At a given non-dimensional position $y$ in the target, $v(y,\tau)$ and $\sigma(y,\tau)$ suffer jump discontinuities at those non-dimensional instants $\tau \geqslant 0$ for which either $\lfloor (\tau - y)/2 \rfloor$ or $\lfloor (\tau + y)/2 \rfloor$ jump to the next integer value.

To shorten subsequent expressions, we will use an abbreviated notation for the exponents in (70) and (71). By (28) and (35) (see also (39)), we have

$$\frac{\tau \pm y}{2} = \frac{t \pm x/c_1}{2t_*} = \frac{c_1 t \pm x}{2l}. \tag{72}$$

Let

$$\mathsf{M}(y,\tau) \equiv \left\lfloor \frac{\tau + y}{2} \right\rfloor = \left\lfloor \frac{t + x/c_1}{2t_*} \right\rfloor = \left\lfloor \frac{c_1 t + x}{2l} \right\rfloor \equiv M(x,t), \tag{73}$$

and

$$\mathsf{N}(y,\tau) \equiv \left\lfloor \frac{\tau - y}{2} \right\rfloor + 1 = \left\lfloor \frac{t - x/c_1}{2t_*} \right\rfloor + 1 = \left\lfloor \frac{c_1 t - x}{2l} \right\rfloor + 1 \equiv N(x,t). \tag{74}$$

$\mathsf{M}(y,\tau)$ and $\mathsf{N}(y,\tau)$ are piecewise-constant, integer-valued functions of $y$ and $\tau$ which, for fixed $y$, are nondecreasing functions of $\tau$. While these functions are well-defined for all real $y$ and $\tau$, for use in (70) and (71) we consider only their values for $\tau \geqslant 0$ and $0 \leqslant y \leqslant 1$.

On rearranging the terms in (70) and (71) and using (73) and (74), we obtain

$$v(y,\tau) = \frac{1}{1-A}\left[1 - b - A^{\mathsf{N}(y,\tau)} + bA^{\mathsf{M}(y,\tau)}\right], \tag{75}$$

$$\sigma(y,\tau) = \frac{1}{1-A}\left[1 + b - A^{\mathsf{N}(y,\tau)} - bA^{\mathsf{M}(y,\tau)}\right]. \tag{76}$$

From (42) we have

$$A = \frac{z_0 - z_1}{z_0 + z_1}\frac{z_2 - z_1}{z_2 + z_1}, \quad b = \frac{z_2 - z_1}{z_2 + z_1}. \tag{77}$$

It follows that

$$1 - A = \frac{2z_1}{z_1 + z_2}\frac{z_0 + z_2}{z_0 + z_1}, \qquad 1 - b = \frac{2z_1}{z_1 + z_2}, \quad 1 + b = \frac{2z_2}{z_1 + z_2}. \tag{78}$$

### 4.6. Expressions for the velocity and stress in the target

From the non-dimensionalization (36), we see that the particle velocity $v_1$ and stress $\sigma_1$ are related to the non-dimensional velocity and stress, $v$ and $\sigma$, by

[7] The ceiling function $\lceil\cdot\rceil : \mathbb{R} \to \mathbb{Z}$ is defined by the condition that $\lceil r \rceil$ is the smallest integer greater than or equal to the real number $r$. Any expression involving floor functions, such as (63), can be converted to an equivalent expression in terms of ceiling functions by using the floor-to-ceiling transformation $\lfloor r \rfloor = -\lceil -r \rceil$.

$$v_1(x,t) = V_1\, v(y,\tau), \quad \sigma_1(x,t) = \Sigma_1\, \sigma(y,\tau). \tag{79}$$

Expressions for $v_1(x,t)$ and $\sigma_1(x,t)$ for $0 \leqslant x \leqslant l$ and $t \geqslant 0$ follow from (79), the relations for $v(y,\tau)$ and $\sigma(y,\tau)$ in Section 4.5, and the fact that $\mathsf{M}(y,\tau) = M(x,t)$ and $\mathsf{N}(y,\tau) = N(x,t)$ (see (73) and (74)). For example, from (75) and (76) we obtain

$$v_1(x,t) = \frac{V_1}{1-A}\left[1 - b - A^{N(x,t)} + bA^{M(x,t)}\right], \tag{80}$$

$$\sigma_1(x,t) = \frac{\Sigma_1}{1-A}\left[1 + b - A^{N(x,t)} - bA^{M(x,t)}\right]. \tag{81}$$

The piecewise-constant, integer-valued functions $M(x,t)$ and $N(x,t)$ are nondecreasing functions of $t$ for fixed $x$. Additional properties of these functions are derived in Section 5.1. For comparison with the concise expressions (80), (81), we state the solutions in the more traditional form of an infinite series of Heaviside functions:

$$v_1(x,t) = V_1 \sum_{n=0}^{\infty} A^n [H(t - t_1) - bH(t - t_2)], \tag{82}$$

$$\sigma_1(x,t) = \Sigma_1 \sum_{n=0}^{\infty} A^n [H(t - t_1) + bH(t - t_2)]. \tag{83}$$

where

$$t_1 = \frac{2ln + x}{c_1}, \quad t_2 = \frac{2l(n+1) - x}{c_1}. \tag{84}$$

These can be obtained by substituting the series solutions (57) and (58) for $F$ and $G$ into (41) and using (79).

Recall that $A$ and $b$ are given by (77), $1 \pm b$ and $1 - A$ by (78), and $V_1$ and $\Sigma_1$ by (26). Alternative expressions for the leading coefficients in (80) and (81) are given by

$$\begin{aligned} \frac{V_1}{1-A} &= \frac{z_0}{z_1}\frac{z_1+z_2}{z_0+z_2}\frac{V_0}{2}, \\ \frac{\Sigma_1}{1-A} &= z_1\frac{V_1}{1-A} = z_0\frac{z_1+z_2}{z_0+z_2}\frac{V_0}{2}. \end{aligned} \tag{85}$$

For the next set of results, it is convenient to introduce the terms

$$V_\infty \equiv \frac{z_0}{z_0+z_2} V_0 = \frac{z_0+z_1}{z_0+z_2} V_1, \tag{86}$$

$$\Sigma_\infty \equiv z_2 V_\infty = \frac{z_0 z_2}{z_0+z_2} V_0 = \frac{z_0+z_1}{z_0+z_2}\frac{z_2}{z_1}\Sigma_1, \tag{87}$$

where the expressions on the right follow from (26). Clearly, $V_\infty$ and $\Sigma_\infty$ are positive; in Section 6.1 we will show that they are the long time asymptotes of velocity and stress in the target. On substitution of $(77)_2$, $(78)_{2,3}$, (85)–(87) into (80) and (81), we obtain the concise expressions

$$v_1(x,t) = \frac{V_\infty}{2}\left[2 - \left(\frac{z_2}{z_1}+1\right)A^{N(x,t)} + \left(\frac{z_2}{z_1}-1\right)A^{M(x,t)}\right], \tag{88}$$

$$\sigma_1(x,t) = \frac{\Sigma_\infty}{2}\left[2 - \left(\frac{z_1}{z_2}+1\right)A^{N(x,t)} + \left(\frac{z_1}{z_2}-1\right)A^{M(x,t)}\right]. \tag{89}$$

## 5. Solutions on either side of the shock

The concise relations for the velocity and stress in Section 4.6 are valid for all times $t \geqslant 0$ and all points $0 \leqslant x \leqslant l$ in the target. We begin this section by evaluating the exponents $M(x,t)$ and $N(x,t)$ in these relations. These results are used in 5.2 to determine the position of the shock at each instant and in Section 5.3 to evaluate the velocity and stress on either side of the shock. In Appendix A we use the results in Sections 3–5 to derive several expressions for the jumps in velocity and stress across the shock.

### 5.1. Evaluation of the exponents $M(x,t)$ and $N(x,t)$

We begin by determining the subsets of the $(x,t)$ plane on which the integer-valued functions $M(x,t)$ and $N(x,t)$ are constant. Let $m$ be any integer. From the definition (73), we see that

$$M(x,t) = m \tag{90a}$$

$$\iff \left\lfloor \frac{t + x/c_1}{2t_*} \right\rfloor = m \tag{90b}$$

$$\iff m \leqslant \frac{t + x/c_1}{2t_*} < m + 1 \tag{90c}$$

$$\iff 2mt_* - x/c_1 \leqslant t < 2(m+1)t_* - x/c_1 \tag{90d}$$

$$\iff c_1(2mt_* - t) \leqslant x < c_1[2(m+1)t_* - t]. \tag{90e}$$

From the definition (74), we see that

$$N(x,t) = m \tag{91a}$$

$$\iff \left\lfloor \frac{t - x/c_1}{2t_*} \right\rfloor = m - 1 \tag{91b}$$

$$\iff m - 1 \leqslant \frac{t - x/c_1}{2t_*} < m \tag{91c}$$

$$\iff 2(m-1)t_* + x/c_1 \leqslant t < 2mt_* + x/c_1 \tag{91d}$$

$$\iff c_1(t - 2mt_*) < x \leqslant c_1[t - 2(m-1)t_*]. \tag{91e}$$

To simplify the subsequent discussion of these results, we introduce abbreviations for some of the expressions above (the arrow superscripts will be motivated in the next subsection):

$$\begin{aligned} s_m^{\leftarrow}(x) &\equiv 2mt_* - x/c_1 = (2m - x/l)t_*, \\ s_m^{\rightarrow}(x) &\equiv 2(m-1)t_* + x/c_1 = [2(m-1) + x/l]t_*, \end{aligned} \tag{92}$$

and

$$\begin{aligned} S_m^{\leftarrow}(t) &\equiv c_1(2mt_* - t) = 2ml - c_1 t, \\ S_m^{\rightarrow}(t) &\equiv c_1[t - 2(m-1)t_*] = c_1 t - 2(m-1)l. \end{aligned} \tag{93}$$

Observe that

$$\begin{aligned} t = s_m^{\leftarrow}(x) &\iff x = S_m^{\leftarrow}(t), \\ t = s_m^{\rightarrow}(x) &\iff x = S_m^{\rightarrow}(t). \end{aligned} \tag{94}$$

Using (92) and (93), we can rewrite the bottom two equivalences in (90) and (91) as

$$\begin{aligned} M(x,t) = m &\iff s_m^{\leftarrow}(x) \leqslant t < s_{m+1}^{\leftarrow}(x), \\ &\iff S_m^{\leftarrow}(t) \leqslant x < S_{m+1}^{\leftarrow}(t), \\ N(x,t) = m &\iff s_m^{\rightarrow}(x) \leqslant t < s_{m+1}^{\rightarrow}(x), \\ &\iff S_{m+1}^{\rightarrow}(t) < x \leqslant S_m^{\rightarrow}(t). \end{aligned} \tag{95}$$

The relations (90)–(95) are valid for any real numbers $x$ and $t$. However, the expressions (80), (81) and (88), (89) for the velocity and stress in the target are only valid for

$$0 \leqslant x \leqslant l \quad \text{and} \quad t \geqslant 0. \tag{96}$$

These restrictions are assumed in the sequel. A graphical representation of the inequalities (95) and (96) is given in Figs. 2 and 3.

Subject to the restrictions (96), for $m = 1, 2, 3, \ldots$ the set of points in the $(x,t)$ plane given by $t = s_m^{\leftarrow}(x)$ is the $m$th line of jump discontinuity of the function $M$; similarly, $t = s_m^{\rightarrow}(x)$ is the $m$th line of jump discontinuity of the function $N$. These lines intersect only at $x = 0$ and $x = l$, that is, at the front and back faces of the target.

For $x = 0$ this occurs at $t = 2t_*, 4t_*, 6t_*, \ldots$; for $x = l$ the intersections occur at $t = t_*, 3t_*, 5t_*, \ldots$.

### 5.2. The shock wave

Since $|A| < 1$, it follows that $A^{M(x,t)}$ and $A^{N(x,t)}$ suffer jump discontinuities along the same lines in the $(x,t)$ plane as the exponents $M$ and $N$. From the relations (80) and (81) or (88) and (89), these are also the lines of jump discontinuity of $v_1(x,t)$ and $\sigma_1(x,t)$ in the $(x,t)$ plane. In other words, the locus of the shock in the $(x,t)$ plane is the union of the lines $t = s_m^{\rightarrow}(x)$ and $t = s_m^{\leftarrow}(x)$ (equivalently, the lines $x = S_m^{\rightarrow}(t)$ and $x = S_m^{\leftarrow}(t)$), subject to the restrictions (96), as $m$ ranges over all positive integers. This is illustrated in Fig. 4.[8]

The line $x = S_m^{\rightarrow}(t)$ has positive slope and represents the $m$th *forward propagating shock* ($m = 1, 2, 3, \ldots$). Note that the forward direction is to the right when the target is oriented as in Fig. 1; hence the right arrows. The line $x = S_m^{\leftarrow}(t)$ has negative slope and represents the $m$th *backward propagating shock* ($m = 1, 2, 3, \ldots$). The backward direction is to the left when the target is oriented as in Fig. 1; hence the left arrows. The changes in the direction of propagation of the shock at $t = t_*, 3t_*, 5t_*, \ldots$ and $t = 2t_*, 4t_*, 6t_*, \ldots$ are due to reflection from the back and front faces of the target, respectively. The triangular shaped regions in Fig. 4 are the regions in which both $M$ and $N$ are constant. The relations

$$\begin{aligned} &N(x,t) \geqslant M(x,t) \geqslant 0, \\ &N(x,t) = M(x,t) \quad \text{or} \quad M(x,t) + 1, \end{aligned} \tag{97}$$

are evident in this figure and also in Figs. 2 and 3; analogous relations hold for the functions $\mathsf{M}(y,\tau)$ and $\mathsf{N}(y,\tau)$ in (73) and (74). By (80) and (81) or (88) and (89), it follows that the triangular regions in Fig. 4 are also regions of constant velocity and stress. As indicated in the figure, $V_0^R, V_1^R, V_2^R, \ldots$ and $\Sigma_0^R, \Sigma_1^R, \Sigma_2^R, \ldots$ denote the sequences of (constant) velocity and stress values to the right of the shock; $V_1^L, V_2^L, V_3^L, \ldots$ and $\Sigma_1^L, \Sigma_2^L, \Sigma_3^L, \ldots$ denote the sequences of (constant) velocity and stress values to the left of the shock. Simple expressions for these values will be derived in the next subsection. The sequences of velocity and stress values at a fixed point $x$ in the *interior* of the target are $V_0^R = 0, V_1^L, V_1^R, V_2^L, V_2^R, \ldots$ and $\Sigma_0^R = 0, \Sigma_1^L, \Sigma_1^R, \Sigma_2^L, \Sigma_2^R, \ldots$, with $V_1^L = V_1$ and $\Sigma_1^L = \Sigma_1$, as will be shown in the next subsection. On the other hand, the sequences of velocity and stress values at the *front face* of the target are $V_1^L, V_2^L, V_3^L, \ldots$ and $\Sigma_1^L, \Sigma_2^L, \Sigma_3^L, \ldots$; and at the *rear face* they are $V_0^R = 0, V_1^R, V_2^R, \ldots$ and $\Sigma_0^R = 0, \Sigma_1^R, \Sigma_2^R, \ldots$.

The results described above are expected on physical grounds. A shock is generated at the front face of the target at the moment of impact: $t = \tau = 0$. It travels at the characteristic (or acoustic) wave speed $c_1$ of the target material,[9] and arrives at the back face of the target at $t = t_* = l/c_1$, the travel time (equivalently, at the non-dimensional time $\tau = 1$). The shock reflects off the back face and arrives at the front face of the target at $t = 2t_*$ (equivalently, $\tau = 2$). Thus the shock completes its first round trip in the target during the time interval $I_1 : 0 \leqslant t \leqslant 2t_*$ (equivalently, $0 \leqslant \tau \leqslant 2$). The shock then reflects off the front face and completes a second round trip during the time interval $I_2 : 2t_* \leqslant t \leqslant 4t_*$ (equivalently, $2 \leqslant \tau \leqslant 4$), and so on for all $t \geqslant 0$. The $m$th round trip of the shock wave ($m = 1, 2, 3, \ldots$) occurs during the time interval

$$I_m : 2(m-1)t_* \leqslant t \leqslant 2mt_*. \tag{98}$$

[8] An exception to the results in this paragraph occurs for the special case $A = 0$. Note that by (42) or (77), $b = 0$ implies $A = 0$.

[9] This property does not extend to nonlinear elastic materials, for which the shock speed depends on the strength of the shock.

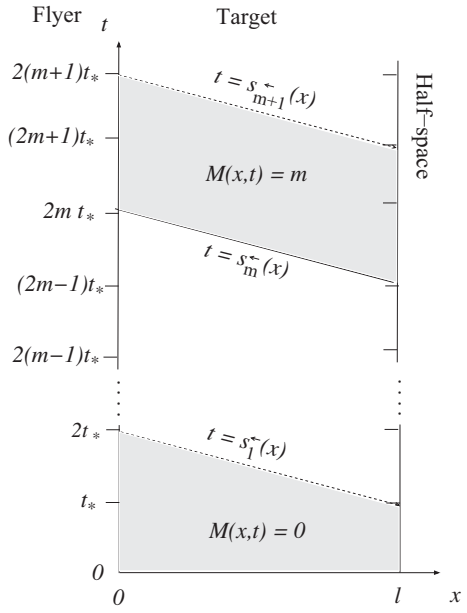


**Fig. 2.** Regions of the $(x,t)$ plane in which the integer-valued functions $M$ are constant. The values indicated are assumed on the solid lines but not on the dashed lines.

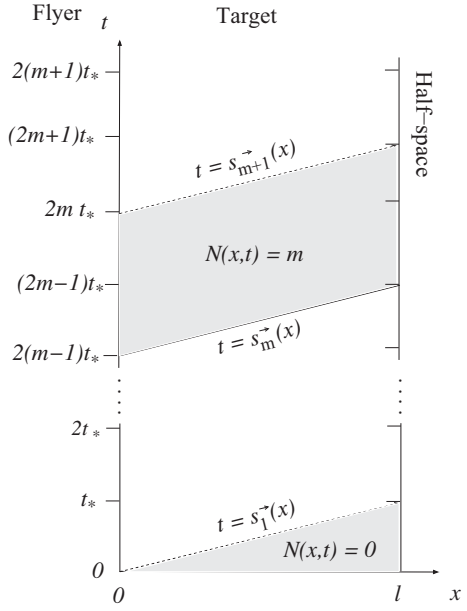


**Fig. 3.** Regions of the $(x,t)$ plane in which the integer-valued functions $N$ are constant. The values indicated are assumed on the solid lines but not on the dashed lines.

We also will refer to this interval itself as the "$m$th round trip". Aside from the instants $2(m-1)t_*, (2m-1)t_*$ and $2mt_*$ at which the shock is at the boundary of the target, $I_m$ is the union of the open subintervals

$$\begin{aligned} &I_m^{\rightarrow} : 2(m-1)t_* < t < (2m-1)t_*, \\ &I_m^{\leftarrow} : (2m-1)t_* < t < 2mt_*. \end{aligned} \tag{99}$$

These time intervals are illustrated on the right side of Fig. 4. For $t \in I_m^{\rightarrow}$ (i.e., during the first half of the $m$th round trip), the shock is propagating forward with position $S_m^{\rightarrow}(t)$ given by (93); the region of the target to the right of the shock (which is ahead of it) has

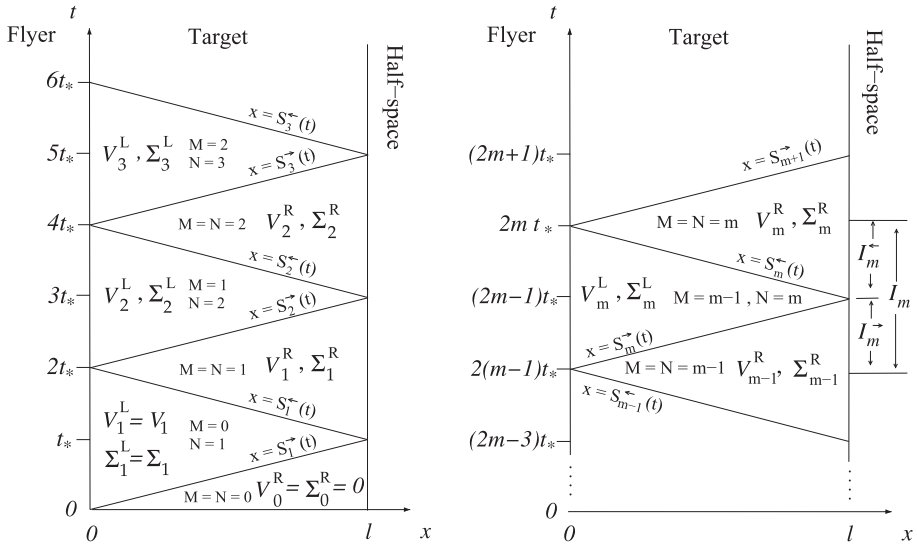


**Fig. 4.** Locus of the shock front in the $(x,t)$ plane. $M$ and $N$ are both constant in the triangular shaped regions, and consequently so are the velocity and stress. $V_m^R$ and $\Sigma_m^R$ $(m=0,1,2,\ldots)$ are the values of the velocity and stress to the right of the shock. $V_m^L$ and $\Sigma_m^L$ $(m=1,2,3,\ldots)$ are the values of the velocity and stress to the left of the shock.

velocity $V_{m-1}^R$ and stress $\Sigma_{m-1}^R$; and the region to the left of the shock (which is behind it) has velocity $V_m^L$ and stress $\Sigma_m^L$. For $t\in I_m^{\leftarrow}$ (i.e., during the second half of the $m$th round trip), the shock is propagating backward with position $S_m^{\leftarrow}(t)$ given by (93); the region of the target to the right of the shock (which is behind it) has velocity $V_m^R$ and stress $\Sigma_m^R$; and the region to the left of the shock (which is ahead of it) still has velocity $V_m^L$ and stress $\Sigma_m^L$, since the reflected shock has yet to alter this state. Finally, from the results in the previous subsection it follows that the left values of velocity and stress hold *on the forward propagating shock,* and the right values of velocity and stress hold *on the backward propagating shock*; however, as discussed in Section 2.3, values assigned to the shock have no real physical significance.

### 5.3. Expressions for the velocity and stress on either side of the shock

From Fig. 4 it follows that the $m$th values of the velocity and stress on the right side of the shock, $V_m^R$ and $\Sigma_m^R$, are obtained by setting $M(x,t)=N(x,t)=m$ in the relations for $v_1(x,t)$ and $\sigma_1(x,t)$ in Section 4.6. In particular, on using (88) and (89) and observing that the impedance ratios cancel, we obtain the following relations (for $m=0,1,2\ldots$):

$$V_m^R=V_\infty(1-A^m),\quad \Sigma_m^R=\Sigma_\infty(1-A^m)=z_2V_m^R. \tag{100}$$

The relation $\Sigma_m^R=z_2V_m^R$ follows from the fact that $\Sigma_\infty=z_2V_\infty$ (see $(87)_1$). Also, recall that expressions for $V_\infty$ in terms of $V_0$ or $V_1$ are given in (86), and expressions for $\Sigma_\infty$ in terms of $V_0$ or $\Sigma_1$ are given in (87). Similarly, from Fig. 4 we see that the $m$th values of the velocity and stress on the *left* side of the shock, $V_m^L$ and $\Sigma_m^L$, are obtained by setting $M(x,t)=m-1$ and $N(x,t)=m$ in the relations for $v_1(x,t)$ and $\sigma_1(x,t)$ in (88) and (89). This yields the following relations (for $m=1,2,3,\ldots$):

$$V_m^L=V_\infty\left(1+\frac{z_2-z_1}{z_0+z_1}A^{m-1}\right)=V_1\left(\frac{z_0+z_1}{z_0+z_2}+\frac{z_2-z_1}{z_2+z_0}A^{m-1}\right), \tag{101}$$

$$\Sigma_m^L=\Sigma_\infty\left(1-\frac{z_2-z_1}{z_0+z_1}\frac{z_0}{z_2}A^{m-1}\right)=\Sigma_1\left(\frac{z_0+z_1}{z_0+z_2}\frac{z_2}{z_1}-\frac{z_2-z_1}{z_2+z_0}\frac{z_0}{z_1}A^{m-1}\right). \tag{102}$$

In deriving these relations, we used the identities

$$\frac{1}{2}\left(\frac{z_2}{z_1}-1\right)-\frac{1}{2}\left(\frac{z_2}{z_1}+1\right)A=\frac{z_2-z_1}{z_0+z_1}, \tag{103}$$

$$\frac{1}{2}\left(\frac{z_1}{z_2}+1\right)A-\frac{1}{2}\left(\frac{z_1}{z_2}-1\right)=\frac{z_2-z_1}{z_0+z_1}\frac{z_0}{z_2}. \tag{104}$$

The expressions on the right in (101) and (102) follow from (86) and (87).

On setting $m=0$ in (100) and using $A^0=1$ (see (66)), we see that

$$V_0^R=\Sigma_0^R=0, \tag{105}$$

as indicated in Fig. 4. That is, the region ahead of the first forward propagating shock is stress-free and at rest, consistent with the initial conditions. On setting $m=1$ in the expressions on the right (101), (102) and using $A^0=1$, we find that

$$V_1^L=V_1\quad\text{and}\quad\Sigma_1^L=\Sigma_1, \tag{106}$$

as indicated in Fig. 4. That is, during the first round trip of the shock the region to the left of the shock has velocity $V_1$ and stress $\Sigma_1$ given by (26). In particular, the conditions (24) and (25) on the front face of the target hold for $t<2t_*$, as claimed in Section 3.4.

On setting $m=1$ in (100), we obtain the relations on the left below and also the relation on the far right for $\Sigma_1^R$:

$$V_1^R=V_\infty(1-A)=\frac{2z_1}{z_1+z_2}V_1=\frac{2z_0z_1}{(z_0+z_1)(z_1+z_2)}V_0>0, \tag{107}$$

$$\Sigma_1^R=\Sigma_\infty(1-A)=\frac{2z_2}{z_1+z_2}\Sigma_1=\frac{2z_0z_1z_2}{(z_0+z_1)(z_1+z_2)}V_0=z_2V_1^R>0. \tag{108}$$

Then the expressions for $V_1^R$ and $\Sigma_1^R$ in terms of $V_1$ follow from (86), (87) and $(78)_1$, and the expressions in terms of $V_0$ follow from (26).

## 6. Additional properties of the solutions

Throughout this section we continue to assume that $z_0,z_1$, and $z_2$ are positive and finite. The limiting cases $z_2\to 0$ or $\infty$ are considered in Section 7.

### 6.1. Long time asymptotes of velocity and stress

Let $x$ be any point in the target. Recall that $M(x,t)$ and $N(x,t)$ are given by (73) and (74). Clearly,

$$M(x,t) \to \infty \quad \text{and} \quad N(x,t) \to \infty \quad \text{as} \quad t \to \infty. \tag{109}$$

Since $|A| < 1$, it follows that

$$A^{M(x,t)} \to 0 \quad \text{and} \quad A^{N(x,t)} \to 0 \quad \text{as} \quad t \to \infty. \tag{110}$$

Now refer to the expressions (88) and (89) for the velocity and the stress. On taking the limit as $t \to \infty$ and using (110), we see that

$$v_1(x,t) \to V_\infty > 0 \quad \text{and} \quad \sigma_1(x,t) \to \Sigma_\infty > 0 \quad \text{as} \quad t \to \infty. \tag{111}$$

Thus $V_\infty$ and $\Sigma_\infty$ are the long time asymptotes of velocity and stress in the target. This conclusion also follows from (100)–(102). From (86) and (87) we see that $V_\infty$ and $\Sigma_\infty$ depend only on the impact speed $V_0$ and the impedances of the flyer and backing material. *It follows that at all points in the target, the long time asymptotes of the velocity and stress are positive and independent of the properties of the target.*[10]

Since the times $t$ in the $m$th round trip $I_m$ of the shock (cf. (98)) approach $\infty$ as $m \to \infty$, and since $|A| < 1$, from the jump conditions in Appendix A we conclude that

$$[[v_1]](t) \to 0 \quad \text{and} \quad [[\sigma_1]](t) \to 0 \quad \text{as} \quad t \to \infty. \tag{112}$$

This result also follows directly from (A.4) and (110).

### 6.2. Sign of the velocity and stress

During the first round trip of the shock, the velocity and stress to the right of the shock are zero when the wave is propagating forward, that is for $0 < t < t_*$ (see Fig. 4 or (105)). However, *for $t > t_*$ and for all points $x$ to the right of the shock, we have $v_1(x,t) > 0$ and $\sigma_1(x,t) > 0$, that is, the particle velocity is in the direction of impact and the stress is compressive.* Indeed, for $t > t_*$ the velocity and stress to the right of the shock take on the sequence of values $V_1^R, V_2^R, \ldots$ and $\Sigma_1^R, \Sigma_2^R, \ldots$, as determined by (100). Since $|A| < 1$ and $V_\infty$ and $\Sigma_\infty$ are positive, it follows that

$$V_m^R > 0 \quad \text{and} \quad \Sigma_m^R > 0 \quad \text{for} \quad m = 1,2,3,\ldots. \tag{113}$$

From (106) the velocity $V_1^L = V_1$ and stress $\Sigma_1^L = \Sigma_1$ to the *left* of the shock during the first round trip are positive, a result which is to be expected for the impact problem considered here. On the other hand, the sign of $V_m^L$ and $\Sigma_m^L$ for $m > 1$ is not so obvious. For those cases where wave reflections would have resulted in separation of the flyer and target if such separation had been permitted, we expect that the"welding" condition will result in a temporary[11] state of tensile stress at the flyer-target interface as well as at all points to the left of the shock. The problem that we now address is to determine the conditions under which this can occur.

For the remainder of this section we assume that $t > 2t_*$ and hence that $t \in I_m$ for some integer $m \geqslant 2$. The stress $\Sigma_m^L$ to the left of the shock is given by (102), and it follows that $\Sigma_m^L < 0$ if and only if

$$\frac{z_2 - z_1}{z_0 + z_1}\frac{z_0}{z_2} A^{m-1} > 1. \quad \text{(tensile stress criterion)} \tag{114}$$

Clearly, this condition requires that $z_2 \neq z_1$ and $A \neq 0$. Since $A$ can be positive or negative depending on the relative magnitudes of the impedances (see $(77)_1$), there would seem to be three cases to consider: (1) $z_2 > z_1$ and $A > 0$ ; (2) $z_2 > z_1$ and $A < 0$, in which case $A^{m-1}$ must be positive, and hence $m$ odd; (3) $z_2 < z_1$ and $A < 0$, in which case $A^{m-1}$ must be negative, and hence $m$ even. However, we can rule out the first two cases. By (A.3), $\Sigma_m^L = \Sigma_{m-1}^R + \Sigma_1 A^{m-1}$ for $t \in I_m^{\rightarrow}$. Since $\Sigma_1 > 0$ and since $\Sigma_{m-1}^R > 0$ for $m \geqslant 2$ (as shown in the first paragraph above), we see that a necessary (but not sufficient) condition for $\Sigma_m^L < 0$ when $m \geqslant 2$ is that $A^{m-1} < 0$, which is possible if and only if $A < 0$ and $m$ is even. This rules out cases (1) and (2) above. Now restrict attention to case (3):

$$z_2 < z_1, \quad A < 0, \quad m \in \{2,4,6,\ldots\}. \tag{115}$$

We claim that if $\Sigma_n^L < 0$ for some $n \in \{4,6,\ldots\}$, then in fact $\Sigma_m^L < 0$ for all $m \in \{2,\ldots,n-2\}$. *It follows that if the stress to the left of the shock ever becomes tensile, then it first becomes tensile during (the entire) second round trip of the shock.*[12] To prove this, it suffices to show that if (114) holds for some $m = n \in \{4,6,\ldots\}$, then it holds for all $m \in \{2,\ldots,n-2\}$. But the latter property follows easily from the former since $|A|^{m_1} > |A|^{m_2}$ for $0 < m_1 < m_2$ and $|A| < 1$.

Referring to the expression $(77)_1$ for $A$, we see that the inequalities in (115), together with the assumption that all impedances are positive, are equivalent to the inequalities

$$0 < z_2 < z_1 < z_0. \tag{116}$$

This and the condition that $m \geqslant 2$ is even are necessary but not sufficient for $\Sigma_m^L < 0$. A necessary and sufficient condition is obtained by determining the additional restrictions imposed on $z_0, z_1, z_2$ and $m$ by the inequality (114). We will restrict attention to the case $m = 2$. From the result in the previous paragraph, we know that if (114) holds for some even $m > 2$ then it is necessarily holds for $m = 2$. To put this another way, satisfaction of (114) for $m = 2$ is necessary (but not sufficient) for (114) to hold for other even values of $m > 2$.

For $m = 2$, the inequality (114) reduces to

$$\frac{z_2 - z_1}{z_0 + z_1}\frac{z_0}{z_2} A > 1; \tag{117}$$

and substitution of the expression $(77)_1$ for $A$ yields, after some algebraic manipulations, the equivalent inequality

$$p(z_{10}) < 0, \quad p(z) \equiv z^2 - (1 - z_{20})z + 3z_{20}, \tag{118}$$

where

$$z_{10} \equiv z_1/z_0, \quad z_{20} \equiv z_2/z_0. \tag{119}$$

Then the inequalities (116) are equivalent to

$$0 < z_{20} < z_{10} < 1. \tag{120}$$

Since the graph of $p(z)$ is concave up, $p(z)$ can take on negative values if and only if it has two distinct real roots, say $z_- < z_+$, in which case $p(z_{10}) < 0$ if and only if

$$z_- < z_{10} < z_+. \tag{121}$$

The roots $z_\pm$ of $p(z)$ depend on $z_{20}$ and are given by

$$2z_\pm = 1 - 2z_{20} \pm \sqrt{q(z_{20})}, \quad q(z) \equiv z^2 - 14z + 1. \tag{122}$$

These roots are real and distinct if and only if $q(z_{20}) > 0$. The roots of $q(z)$ are $7 \pm 4\sqrt{3}$. Since the graph of $q(z)$ is concave up, $q(z_{20}) > 0$ if and only if $z_{20} < 7 - 4\sqrt{3}$ or $z_{20} > 7 + 4\sqrt{3}$. But the latter inequality violates (120), so we must have

$$0 < z_{20} < 7 - 4\sqrt{3} < 0.071797. \tag{123}$$

[10] As will be shown in Sections 7.1 and 7.2, this conclusion is also true if the back face of the target is either stress-free or rigidly fixed, with the exception that $\Sigma_\infty = 0$ in the former case and $V_\infty = 0$ in the latter case.

[11] That this tensile state is necessarily temporary follows from (111).

[12] If the assumption that the flyer and target weld on impact were not imposed, then a tensile stress cannot be supported at the front face of the target. Consequently, separation of the flyer and target, if it occurs at all, would necessarily occur at $t = t_c = 2t*$.

Summarizing, we have shown that $p(z_{10}) < 0$ if and only if (123) and (121) hold, provided that the middle and right inequalities in (120) are also satisfied in this case. This turns out to be the case, although we omit the proof. Then from the earlier discussion it follows that $\Sigma_2^L < 0$ *(that is, the stress to the left of the shock is tensile during the second round trip*: $2t_* < t < 4t_*$*) if and only if the impedance ratio* $z_{20} \equiv z_2/z_0$ *satisfies* (123) *and the impedance ratio* $z_{10} \equiv z_1/z_0$ *satisfies* (121)*, with* $z_\pm$ *determined by* $z_{20}$ *as in* (122). Once $z_{20}$ and $z_{10}$ have been chosen to satisfy these conditions, all three impedance ratios are determined since $z_1/z_2 = z_{10}/z_{20}$; hence, the selection of $z_{20}, z_{10}$ and one of the impedances determines all three impedances. For example, $z_{20} = 1/20$ satisfies (123). Then $\sqrt{q(z_{20})} = 11/20, z_- = 1/5$ and $z_+ = 3/4$, so that (121) is satisfied if we take $z_{10} = 1/2$. If we choose $z_1 = 1$, then $z_0 = z_1/z_{10} = 2$, and $z_2 = z_{20}z_0 = 1/10$, and for this set of impedances $\Sigma_2^L < 0$. A plot of the stress and velocity histories at the impact face for an impact problem with this particular set of impedances is given in Section 8.

## 7. Solutions for special cases of the impedance

In this section we consider the special cases $z_2 = 0$ (Section 7.1), and $z_2 = \infty$ (Section 7.2). The analysis up to this point has also assumed that $z_2$ is positive and finite, so the results for the cases $z_2 = 0$ and $z_2 = \infty$ are obtained by taking limits of our earlier results as $z_2$ approaches zero or infinity.

### 7.1. Target with stress-free back face ($z_2 = 0$)

In this section, we derive solutions for the impact problem when the back face of the target is stress-free:

$$\sigma_1(l,t) = 0, \quad t \in \mathbb{R}. \tag{124}$$

This boundary condition corresponds to the case where there is no backing material; it also follows from the back face boundary condition (32) in the limit as

$$z_2 \to 0. \tag{125}$$

Consequently, the appropriate relations for the stress and velocity in the target for the stress-free boundary condition (124) can be obtained by taking the limit of the results in Sections 4–6 as $z_2 \to 0$. [13]. From (42) we see that $a$ is unchanged as $z_2 \to 0$, whereas

$$b \to -1, \quad A \to -a = \frac{z_1 - z_0}{z_1 + z_0} \tag{126}$$

in this case. By (85)–(87), we see that as $z_2 \to 0$,

$$\frac{V_1}{1-A} \to \frac{V_0}{2}, \quad \frac{\Sigma_1}{1-A} \to z_1 \frac{V_0}{2}, \quad V_\infty \to V_0, \quad \Sigma_\infty \to 0. \tag{127}$$

On using (126) and $(127)_{1,2}$ in (80) and (81), we see that in the limit as $z_2 \to 0$ the velocity and stress are given by

$$\begin{aligned} v_1(x,t) &= \frac{V_0}{2}\left[2 - A^{N(x,t)} - A^{M(x,t)}\right], \\ \sigma_1(x,t) &= z_1 \frac{V_0}{2}\left[-A^{N(x,t)} + A^{M(x,t)}\right], \end{aligned} \tag{128}$$

for any $t \geqslant 0$ and $0 \leqslant x \leqslant l$, with $A$ as in (126). Here we have used the fact that the nonnegative, piecewise-constant, integer-valued functions $M$ and $N$ defined in (73) and (74) are independent of $z_2$.

[13] Actually, this statement requires proof, as does the analogous statement for the fixed back face ($z_2 \to \infty$) in the next subsection. The solutions for stress-free or fixed back faces can also be derived directly by procedures analogous to those used in Sections 4–6. We have done this, and the results agree with those derived here by taking limits of the back face impedance. This agreement is also corroborated (for two special cases) by the discrete solutions in Section 8.

From (128) and (110), or from (111) and $(127)_{3,4}$, we see that

$$v_1(x,t) \to V_0 > 0 \quad \text{and} \quad \sigma_1(x,t) \to 0 \quad \text{as} \quad t \to \infty. \tag{129}$$

*At all points in the target, the long time asymptote of the velocity is the impact speed of the flyer and the long time asymptote of the stress is zero, independent of the properties of the target.*

Alternative expressions for the stress and velocity hold on either side of the shock. For $m = 0, 1, 2, \ldots$, the $m$th values of velocity and stress on the right side of the shock are obtained from (100) and $(127)_{3,4}$:

$$\Sigma_m^R = 0, \quad V_m^R = V_0\left(1 - A^m\right). \tag{130}$$

Note the zero stress condition above is consistent with the boundary condition (124). For $m = 1, 2, 3, \ldots$, the $m$th values of velocity and stress on the left side of the shock are given by

$$\Sigma_m^L = \Sigma_1 A^{m-1}, \qquad V_m^L = V_0\left(1 - \frac{z_1}{z_0 + z_1} A^{m-1}\right). \tag{131}$$

The expression for $V_m^L$ follows from $(127)_3$ and the relation on the left in (101) as $z_2 \to 0$. The relation for $\Sigma_m^L$ on the left in (102) is indeterminate as $z_2 \to 0$; the relation on the right approaches the result above.

Finally, by $(131)_1$, we see that the stress to the left of the shock is tensile during the $m$th round trip if and only if $A < 0$ and $m$ is even; and by (126), $A < 0$ iff $z_0 > z_1$. Thus if $z_0 > z_1$ then the stress to the left of the shock is tensile during the 2nd, 4th, 6th, ...round trips; see Section 8 for a particular example of this case.

### 7.2. Target with fixed back face ($z_2 = \infty$)

In this section, we derive solutions for the impact problem when the back face of the target is fixed:

$$v_1(l,t) = 0, \quad t \in \mathbb{R}. \tag{132}$$

This boundary condition corresponds to the case where the backing medium is rigid; it follows from the back face boundary condition (32) on dividing by $z_2$ and then taking the limit as

$$z_2 \to \infty. \tag{133}$$

Consequently, the appropriate relations for the stress and velocity in the target for the rigid boundary condition (132) can be obtained by taking the limit of the results in Sections 4–6 as $z_2 \to \infty$. From (42) we see that $a$ is unchanged as $z_2 \to \infty$, whereas

$$b \to 1, \quad A \to a = \frac{z_0 - z_1}{z_0 + z_1} \tag{134}$$

in this case. By (85)–(87), we see that as $z_2 \to \infty$,

$$\frac{V_1}{1-A} \to \frac{z_0}{z_1}\frac{V_0}{2}, \quad \frac{\Sigma_1}{1-A} \to z_0 \frac{V_0}{2}, \quad V_\infty \to 0, \quad \Sigma_\infty \to z_0 V_0. \tag{135}$$

On using (134) and $(135)_{1,2}$ in (80) and (81), we see that in the limit as $z_2 \to \infty$ the velocity and stress are given by

$$\begin{aligned} v_1(x,t) &= \frac{z_0}{z_1}\frac{V_0}{2}\left[-A^{N(x,t)} + A^{M(x,t)}\right], \\ \sigma_1(x,t) &= z_0 \frac{V_0}{2}\left[2 - A^{N(x,t)} - A^{M(x,t)}\right], \end{aligned} \tag{136}$$

for any $t \geqslant 0$ and $0 \leqslant x \leqslant l$, with $A$ as in (134). From (136) and (110), or from (111) and $(135)_{3,4}$, we see that

$$v_1(x,t) \to 0 \quad \text{and} \quad \sigma_1(x,t) \to z_0 V_0 > 0 \quad \text{as} \quad t \to \infty. \tag{137}$$

*At all points in the target, the long time asymptote of the velocity is zero and the long time asymptote of the stress is the product of the impedance and impact speed of the flyer, independent of the properties of the target.*

Alternative expressions for the stress and velocity hold on either side of the shock. For $m = 0, 1, 2, \ldots$, the $m$th values of velocity and stress on the right side of the shock are obtained from (100) and $(135)_{3,4}$:

$$V_m^R = 0, \quad \Sigma_m^R = z_0 V_0 (1 - A^m). \tag{138}$$

Note that the zero velocity condition above is consistent with the boundary condition (132). For $m = 1, 2, 3, \ldots$, the $m$th values of velocity and stress on the left side of the shock are given by

$$V_m^L = V_1 A^{m-1}, \quad \Sigma_m^L = z_0 V_0 \left(1 - \frac{z_0}{z_0 + z_1} A^{m-1}\right). \tag{139}$$

The expression for $\Sigma_m^L$ follows from $(135)_4$ and the relation on the left in (102) in the limit as $z_2 \to \infty$. The relation for $V_m^L$ on the left in (101) is indeterminate as $z_2 \to \infty$; the relation on the right approaches the result above.

Finally, since $|A| < 1$ and $z_0/(z_0 + z_1) < 1$, from (138) and (139) we see that the stress is never tensile in this case.

## 8. Stress and velocity histories for several impact problems

In this section we plot the time histories of the stress and particle velocity at either the front face or the midpoint of the target for four different impact problems. The results are shown in Figs. 5–8. Also included in these figures are the long-time asymptotic relations for the stress and velocity and, for Figs. 5 and 6, the numerical values of these asymptotes. In all four examples the velocity of the flyer is $V_0 = 5$. The Time on the horizontal axis is the non-dimensional time $\tau = t/t_*$. The Time can also be interpreted as the dimensional time $t$ provided that the travel time $t_* = 1$, in which case we must have $l = c_1$ since $t_* = l/c_1$. The stress and velocity values are dimensional, that is, $\sigma_1$ and $v_1$.

Fig. 5 is a plot of the stress and velocity histories at the impact face $(x = 0)$ for flyer, target and backing impedances of $z_0 = 2, z_1 = 1$ and $z_2 = 1/10$, respectively. The histories are calculated from the relations (88) and (89). The impedances are taken from the example at the end of Section 6.2, which is a case for which the stress should temporarily becomes tensile after the first round trip of the shock. As is evident in the figure, the stress is negative, and hence tensile, for non-dimensional times $2 < \tau < 4$. Note that since the stress and velocity at the impact face is not constant

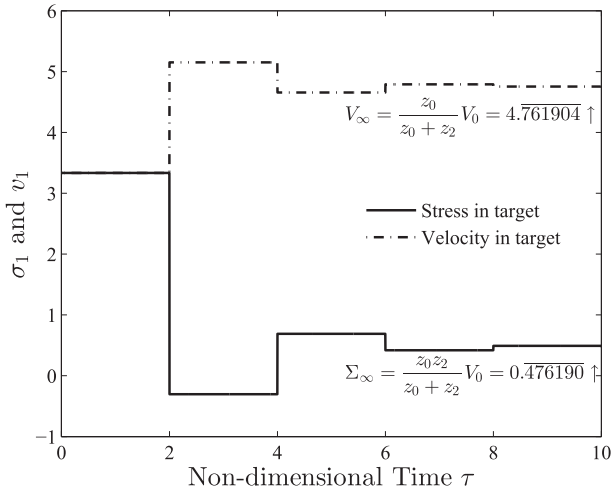


**Fig. 5.** Stress and particle velocity histories at the front face of the target $(x = 0)$ for impact speed $V_0 = 5$. The flyer, target and backing impedances are $z_0 = 2, z_1 = 1$ and $z_2 = 1/10$, respectively. Observe that the stress is tensile for non-dimensional times $2 < \tau < 4$.

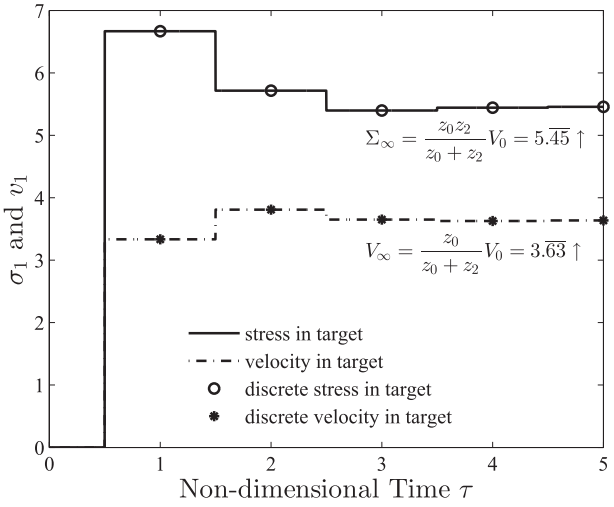


**Fig. 6.** Stress and particle velocity histories at the midpoint of the target $(x = l/2)$ for impact speed $V_0 = 5$. The flyer, target and backing impedances are $z_0 = 4, z_1 = 2$ and $z_2 = 1.5$, respectively.

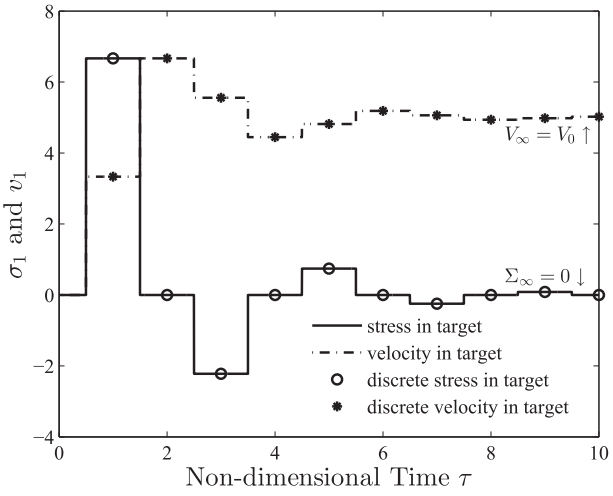


**Fig. 7.** Stress and particle velocity histories at the midpoint of the target $(x = l/2)$ for a stress-free back face. The flyer and target impedances are $z_0 = 4$ and $z_1 = 2$, and the impact speed is $V_0 = 5$.

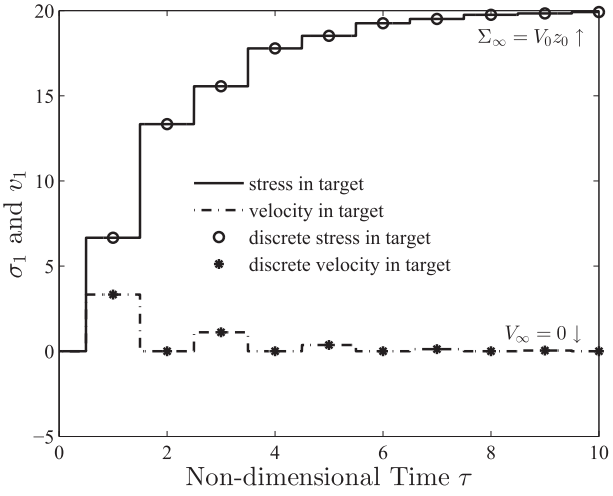


**Fig. 8.** Stress and particle velocity histories at the midpoint of the target $(x = l/2)$ for a rigid back face. The flyer and target impedances are $z_0 = 4$ and $z_1 = 2$, and the impact speed is $V_0 = 5$.

after impact, the common "impact-type" boundary conditions, consisting of a step in stress or velocity at the front face of the target, would provide an incorrect solution to this impact problem. Fig. 6 is for the case of a backing material with impedance $z_2 = 1.5$; the histories are calculated from the relations (88) and (89). Figs. 6–8 are plots of the stress and velocity histories at the midpoint of the target, $x = l/2$, with flyer and target impedances of $z_0 = 4$ and $z_1 = 2$. Fig. 7 is for the case of a stress-free back face, and Fig. 8 is for the case of a rigid back face; the time histories are calculated from the relations (128) and (136), respectively. Since $z_0 > z_1$, the tensile stress during the 2nd and 4th round trips for the stress-free case in Fig. 7 is consistent with the observation at the end of Section 7.1.

In a companion paper (Gazonas and Velo, in preparation), we develop an algorithm for solving impact problems in multilayered media with an arbitrary number of homogeneous layers. The algorithm becomes especially useful for impact problems involving many layers, where explicit analytical solutions may be intractable; see also Gazonas and Velo (2012) and Velo et al. (2009) for related work involving other loading conditions. The algorithm is based on the method of characteristics and involves a coupled system of recursive relations for the sequences of stress and velocity values in the interior[14] of each layer; a discrete version of the impact boundary condition (18) is used. Closed-form solutions of the system of recursive relations are obtained by using the $z$-transform. Figs. 6–8 include the corresponding discrete solutions for the particular impact problems considered in these figures. The figures demonstrate the agreement between the explicit analytical solutions in Sections 4.6 and 7 and the explicit discrete solutions from Gazonas and Velo (in preparation) for all the three back face boundary conditions: a semi-infinite backing medium, a stress-free or fixed back face. In addition, for the cases considered here we have also verified that the analytical and discrete solutions are in agreement with the values for the velocity and stress on either side of the shock obtained from the expressions in Sections 5.3 and 7.[15]

## 9. Discussion and conclusions

We begin with a discussion of other methods (both classical and more recent) for solving the one dimensional wave equation in multilayered, linear elastic media (Sections 9.1 and 9.2). This is followed by a discussion of the techniques used here (Section 9.3).

### 9.1. Time-domain d'Alembert methods

Techniques based on d'Alembert's solution of the one-dimensional wave equation are quite common and have been extremely effective; cf. Goldsmith (2001, p. 38) or Graff (1975, p. 95) for the solution of simplified rod impact problems in linear elastic media. In more recent studies, Rossikhin and Shitikova (2007) considered the thermoelastic rod impact problem using a time-domain d'Alembert formalism. Similar time-domain solutions were developed by Bityurin (2011) who investigated rod stability due to repeated rod impact onto a rigid barrier. Hu et al. (2003) considered the impact problem of a rigid sphere onto a free rod and validated a hybrid St. Venant–Hertz impact model with experimental measurements of strain and velocity at fixed positions in the rods. The problem of wave propagation induced by impact was solved using the d'Alembert method by Yu et al. (2010) and was subsequently used to verify an explicit space time finite-volume scheme for solving linear/nonlinear hyperbolic systems.

### 9.2. Other semi-analytical methods

Analytical methods other than the d'Alembert solution have been used to solve more difficult impact and wave propagation problems, and Laplace transform methods are almost universally applied to transform and simplify the governing equations. In such cases, a number of either analytical or numerical inverse Laplace transform techniques have been used to invert the transformed solutions back into the time-domain. For example, Schwarz et al. (2010) invoked the so-called Laguerre polynomial technique for Laplace transform inversion and derived solutions for rod interactions with deformable barriers applicable to stamping tools, whereas Werner and Fischer (1995) determined the inverse Laplace transform using the method-of-residues for problems involving the sudden arrest of rods in motion. The use of residue calculus and the evaluation of the Bromwich integral (akin to the Heaviside expansion theorem, cf. Fodor (1965, p. 87)) for impact and wave propagation problems results in solutions that exhibit the Gibbs phenomenon (Bracewell, 1965), as they are written in terms of an infinite series of transcendental functions. One may also invoke the method of separation of variables and Fourier analysis by superimposing waves of different wavelengths to generate solutions to the wave equation (Graff, 1975); such methods of superposition are generally inefficient for solving elastodynamic problems with jump discontinuities and they also suffer from the Gibbs phenomenon. More sophisticated integral representation solutions of the wave equation can be derived using a Green's function formalism and often combine both Laplace and Fourier transforms (Graff, 1975; Achenbach, 1984).

Finally, we mention the class of discrete methods for solving the wave equation in multi-layered media which, for certain loading conditions, yield exact solutions. These methods are represented by a set of coupled recursion relations for the stress and velocity in the layers. A variety of recursive solutions to the wave equation have been developed for impact-type problems (Drumheller, 1998; Gazonas and Velo, in preparation), wave propagation and inverse problems arising in geophysics (Bube and Burridge, 1983), resonance phenomena in multilayered media (Gazonas and Velo, 2012), and optimal design problems (Velo et al., 2009).

### 9.3. Combined d'Alembert and Laplace transform methods

Less common are solution methodologies that combine the d'Alembert solution with Laplace transform methods, as illustrated in some recent wave propagation (Hopkins and Gazonas, 2011) and impact (Randow and Gazonas, 2009; Gazonas et al., 2014; Gazonas et al., 2015) studies. This combined analytical approach was employed in the current study.

Two additional features of the current study are the application of an impact boundary condition on the front face of the target and the use of the floor (or greatest integer) function. The impact boundary condition (1), together with the more conventional back face boundary condition (32), allowed us to reduce the impact problem to an initial-boundary value problem for the target alone. Both of these boundary conditions are, with some qualifications, independent of the target properties. The use of the floor function allowed us to express the Heaviside series for the Laplace transform solution of the d'Alembert functions in a simple explicit form. This led to apparently new, compact expressions for the stress and particle velocity in the target which are amenable to long-time asymptotic analysis.

[14] For this reason, the discrete solution is not plotted in Fig. 5.

[15] In Gazonas and Velo (in preparation) we give an algebraic proof that for the impact problems considered in this paper and for arbitrary values of the parameters, the closed-form discrete solutions in Gazonas and Velo (in preparation) are equivalent to the the relations (100)–(102), (130) and (131) or (138) and (139) for the velocity and stress on either side of the shock.

Floor function constructs are used ubiquitously in mathematical programming (Iverson, 1962), number theory (Hardy and Wright, 1979), and related unsolved number-theoretic problems (Guy, 1994). Since a subset of these solutions is exact (i.e., they exhibit no round off error), they form an important contribution to the class of benchmark problems (Idesman et al., 2009) relevant to verification of large-scale computational codes (Oberkampf and Roy, 2010).

Our results are corroborated by discrete solutions of a recursive system of equations, derived in Gazonas and Velo (in preparation), and applied to the impact boundary value problem studied here. On the other hand, the agreement of the two methods provides partial verification of the these recursive methods for this special case. This is important since exact, analytical solutions for a wider class of impact problems involving targets with multiple layers are difficult to obtain.

Our current work in this area indicates that the impact boundary condition (1) is also applicable to the impact of a semi-infinite elastic flyer on a piezoelectric target backed by a semi-infinite elastic half-space (Gazonas et al., 2014). Furthermore, this boundary condition can be modified to apply to both elastic and piezoelectric flyers of *finite* thickness (Gazonas et al., 2015).

The use of floor functions for solving problems in elastodynamics has implications beyond problems involving impact. For example, the classic problem of a finite elastic strip fixed at $x = 0$ with a transient traction $p(t)$ applied at $x = l$, cf. Eringen and Şuhubi (1975, Section 6.6), can also be written in explicit form using floor functions. Also, the solution for a string (with unit wave speed) subjected to a transient displacement $f(t)$ at $x = 0$ with the end $x = l$ allowed to slide freely along a line perpendicular to the undeformed string, cf. Courant and Hilbert (1962, pp. 508–510), is also solvable in terms of floor functions.

## Appendix A. The jumps in stress and velocity across the shock

Let $S(t)$ denote the position of the shock at time $t \geqslant 0$. At an instant $t$ when $S(t)$ is in the interior of the target, that is, $0 < x < l$, the jump in a field variable $\varphi$ across the shock, denoted by $[[\varphi]]$, is defined as follows:

$$[[\varphi]](t) \equiv \lim_{\substack{x \to S(t) \\ \text{frombehindtheshock}}} \varphi(x,t) - \lim_{\substack{x \to S(t) \\ \text{fromaheadoftheshock}}} \varphi(x,t) = \lim_{\tilde{t} \downarrow t} \varphi(S(t),\tilde{t}) - \lim_{\tilde{t} \uparrow t} \varphi(S(t),\tilde{t}). \tag{A.1}$$

The opposite sign convention, that is, $(A.1)_1$ with the two limits interchanged, is also used in some of the literature. The equivalence of these relations is easily seen from Fig. 4 if we recall that for a forward propagating shock, positions $x$ to the right of the shock are ahead of it and positions $x$ to the left of the shock are behind it, while for a backward propagating shock the reverse is true. The relation on the right is also well-defined at an instant $t$ when $S(t)$ is on the front or back face of the target, so this is the definition of the jump that will be used in these cases. Observe that $[[\varphi]]$ is positive (negative) if and only if the value of $\varphi$ behind the shock is larger (smaller) than the value of $\varphi$ ahead of the shock, equivalently, if $\varphi$ increases (decreases) on the passage of the shock. Of course, $[[\varphi]] = 0$ if and only if $\varphi$ is continuous. The shock wave is *compressive (tensile)* at the instant $t$ if $[[\sigma_1]](t)$ is positive (negative), that is, if the stress behind the shock exceeds (is exceeded by) the stress ahead of it. Note that this definition refers to the sign of the jump in stress, not to the signs of the stress on either side of the shock. Now consider the jump in velocity and stress across the shock during the $m$th round trip $I_m$ ($m = 1, 2, 3, \ldots$). Restricting attention to those instants $t$ at which the shock front $S(t)$ lies in the interior of the specimen, we claim that

$$[[v_1]](t) = \begin{cases} V_m^L - V_{m-1}^R &= V_1 A^{m-1}, \quad t \in I_m^{\rightarrow}, \\ &= \frac{z_0}{z_0+z_1} V_0 A^{m-1}, \\ V_m^R - V_m^L &= -bV_1 A^{m-1}, \quad t \in I_m^{\leftarrow}, \\ &= -\frac{z_2-z_1}{z_2+z_1}\frac{z_0}{z_0+z_1} V_0 A^{m-1}, \end{cases} \tag{A.2}$$

$$[[\sigma_1]](t) = \begin{cases} \Sigma_m^L - \Sigma_{m-1}^R &= \Sigma_1 A^{m-1}, \quad t \in I_m^{\rightarrow}, \\ &= \frac{z_0 z_1}{z_0+z_1} V_0 A^{m-1}, \\ \Sigma_m^R - \Sigma_m^L &= b\Sigma_1 A^{m-1}, \quad t \in I_m^{\leftarrow}, \\ &= \frac{z_2-z_1}{z_2+z_1}\frac{z_0 z_1}{z_0+z_1} V_0 A^{m-1}, \end{cases} \tag{A.3}$$

The relations on the left follow immediately from Fig. 4 and the definition (A.1) of the jump. The top expressions on the right can be obtained from the relations (100)–(102) for $V_m^R, \Sigma_m^R, V_m^L$ and $\Sigma_m^L$ after some algebraic manipulations; we can also proceed as in the next paragraph. The bottom expressions on the right follow from $(77)_2$ and (26). From (80) and (81) we see that the jumps in velocity and stress at any time $t \geqslant 0$ are given by

$$\begin{aligned} [[v_1]](t) &= \frac{V_1}{A-1}\left[[[A^N]](t) - b[[A^M]](t)\right], \\ [[\sigma_1]](t) &= \frac{\Sigma_1}{A-1}\left[[[A^N]](t) + b[[A^M]](t)\right]. \end{aligned} \tag{A.4}$$

Consider the case where $t \in I_m^{\rightarrow}$. Then from Figs. 2, 3 or 4, $M(x,t)$ is a continuous function of $x$ and $t$, and (A.4) reduces to

$$[[v_1]](t) = \frac{V_1}{A-1}[[A^N]](t), \quad [[\sigma_1]](t) = \frac{\Sigma_1}{A-1}[[A^N]](t).$$

From Fig. 4 and the definition (A.1) of the jump, we see that $[[A^N]](t) = A^m - A^{m-1} = (A-1)A^{m-1}$, which together with the above relations yields the top middle expressions in (A.2) and (A.3). Similar arguments yield the bottom middle expressions; note that in this latter case $N(x,t)$ is continuous and $M(x,t)$ suffers a jump discontinuity. This completes the proof of (A.2) and (A.3).

From (42) we see that the sign of $A$ depends on the signs of the impedance differences $z_0 - z_1$ and $z_2 - z_1$. Consequently, by (A.2) and (A.3), the signs of the jumps in velocity and stress depend on the signs of these impedance differences and, if $A < 0$, on whether $m$ is even or odd. From the middle or left expressions in (A.2) and (A.3), we see that the jump in velocity (stress) across the backward propagating shocks is a constant multiple, namely $-b$ ($+b$), of the corresponding jump across the forward propagating shocks. Also, from the middle expressions for $[[v_1]](t)$ and $[[\sigma_1]](t)$ and the fact that $\Sigma_1 = z_1 V_1$ (see (26)), or directly form the expressions on the right in (A.2) and (A.3), we see that

$$[[\sigma_1]](t) = \pm z_1 [[v_1]](t) \quad \text{(in the interior of the target)}, \tag{A.5}$$

independent of $m$ and also independent of the properties of the flyer and backing medium. Here the "+" case holds for forward propagating shocks and the "−" case holds for the backward propagating shocks.[16]

From (66) and (A.2)–(A.3) with $m = 1$, or directly from Fig. 4, we see that the jumps in velocity and stress across the first forward propagating shock ($t \in I_1^{\rightarrow} : 0 < t < t_*$) are given by $V_1$ and $\Sigma_1$, respectively. These are also the jumps in velocity and stress at the front face of the target at the moment of impact, $t = 0$. How-

[16] The relation (A.5) can be established independently of (A.2) and (A.3). Since there is no wave reflection during either of the time intervals in question, momentum balance across the shock is given by $[[\sigma_1]] = \rho_1 U_1 [[v_1]]$, where $U_1$ is the shock *velocity* (i.e., the signed speed): $U_1 = \pm c_1$, with the + (−) case holding when the wave in the target is propagating in the positive (negative) $x$ direction.

ever, the definition of the jump on the left side of (A.1) does not apply at the front or back face of the target for times $t > 0$, and the relations (A.2) and (A.3) are not valid there. At the front and back faces, the velocity and stress suffer jumps at any instant when shock reflection occurs, and we apply the expression for the jump on the right in (A.1). For the back face, shock reflection occurs at $t = t_*, 3t_*, 5t_*, \ldots$ (see Fig. 4), and the jumps in velocity and stress at these instants are given by

$$[[v_1]]((2m-1)t_*) = V_m^R - V_{m-1}^R = V_1^R A^{m-1}, \tag{A.6}$$

$$[[\sigma_1]]((2m-1)t_*) = \Sigma_m^R - \Sigma_{m-1}^R = \Sigma_1^R A^{m-1}, \tag{A.7}$$

for $m = 1, 2, 3, \ldots$. Recall that expressions for $V_1^R$ and $\Sigma_1^R$ are given in (107) and (108). For the front face, shock reflection occurs at $t = 2t_*, 4t_*, 6t_*, \ldots$, and the jumps in velocity and stress at these instants are given by

$$[[v_1]](2mt_*) = V_{m+1}^L - V_m^L = \frac{z_1 - z_2}{z_0 + z_1} \cdot V_1^R A^{m-1}, \tag{A.8}$$

$$[[\sigma_1]](2mt_*) = \Sigma_{m+1}^L - \Sigma_m^L = \frac{z_2 - z_1}{z_2 + z_0}\frac{z_0}{z_2} \cdot \Sigma_1^R A^{m-1}, \tag{A.9}$$

for $m = 1, 2, 3, \ldots$. Note that these are constant (i.e., independent of $m$) multiples of the corresponding jumps on the back face. The relations on the left in (A.6)–(A.9) follow easily from Fig. 4. The relations on the right follow from (100)–(102) and (107)–(108). They can also be obtained from (A.4); note that $M$ and $N$ suffer jump discontinuities simultaneously in these cases. Since $\Sigma_1^R = z_2 V_1^R$ (see (108)), the relations (A.6)–(A.9) imply[17] that for $t = t_*, 3t_*, 5t_*, \ldots$,

$$[[\sigma_1]](t) = z_2[[v_1]](t) \quad \text{(on the back face)}; \tag{A.10}$$

and for $t = 2t_*, 4t_*, 6t_*, \ldots$,

$$[[\sigma_1]](t) = -z_0[[v_1]](t) \quad \text{(on the front face)}. \tag{A.11}$$

## References


Achenbach, J.D., 1984. Wave Propagation in Elastic Solids. North-Holland Publishing Company, New York.

Bityurin, A.A., 2011. The loss of stability of a two-step rod when it hits a rigid barrier. Pmm-J. Appl. Math. Mech. 75 (1), 73–76.

Bracewell, R., 1965. The Fourier Transform and Its Applications. McGraw-Hill Book Company, New York.

Bube, K., Burridge, R., 1983. The one dimensional inverse problem of reflection seismology. SIAM Rev. 25 (4), 497559.

Chen, X., Chandra, N., Rajendran, A.M., 2004. Analytical solution to the plate impact problem of layered heterogeneous material systems. Int. J. Solids Struct. 41 (16–17), 4635–4659.

Courant, R., Hilbert, D., 1962. Methods of Mathematical Physics. Partial Differential Equations, Volume II. Interscience Publishers, New York.

Davison, L., 2008. Fundamentals of Shock Wave Propagation in Solids. Springer-Verlag, Heidelberg, Germany.

Dayal, K., Bhattacharya, K., 2006. Kinetics of phase transformations in the peridynamic formulation of continuum mechanics. J. Mech. Phys. Solids 54 (9), 1811–1842.

Doetsch, G., 1974. Introduction to the Theory and Application of the Laplace Transformation. Springer-Verlag, New York.

Drumheller, D.S., 1998. Introduction to Wave Propagation in Nonlinear Fluids and Solids. Cambridge University Press, United Kingdom.

Dutta, A., Tekalur, S.A., Miklavcic, M., 2013. Optimal overlap length in staggered architecture composites under dynamic loading conditions. J. Mech. Phys. Solids 61 (1), 145–160.

Eringen, A.C., Şuhubi, E.S., 1975. Elastodynamics. Linear Theory, vol. II. Academic Press, New York.

Fodor, G., 1965. Laplace Transforms in Engineering. Akadémiai Kiadó, Budapest, Hungary.

Gazonas, G.A., Velo, A.P., 2012. Analytical solutions for the resonance response of Goupillaud-type elastic media using $z$-transform methods. Wave Motion 49, 135–151.

Gazonas, G.A., Velo, A.P., Recursive solutions for elastodynamic impact into multilayered media, in preparation.

Gazonas, G.A., Wildman, R.A., Hopkins, D.A., 2014. Elastodynamic impact into piezoelectric media. U.S. Army Research Laboratory, Aberdeen Proving Ground, MD. ARL-TR-7056, 1–30.

Gazonas, G.A., Wildman, R.A., Hopkins, D.A., Scheidler, M.J., 2015. Longitudinal impact of piezoelectric media. Arch. Appl. Mech. http://dx.doi.org/10.1007/s00419-015-1042-3.

Goldsmith, W., 2001. Impact: The Theory and Physical Behavior of Colliding Solids. Dover Publications, New York.

Graff, K.F., 1975. Wave Motion in Elastic Solids. Dover Publications, New York.

Guy, R.K., 1994. Unsolved Problems in Number Theory. Springer-Verlag, New York.

Hardy, G.H., Wright, E.M., 1979. An Introduction to the Theory of Numbers. Oxford University Press, Oxford.

Hopkins, D.A., Gazonas, G.A., 2011. Wave Propagation in Second-Order Nonlinear Piezoelectric Media. U.S. Army Research Laboratory, Aberdeen Proving Ground, MD. ARL-TR-5766, 1–44.

Hu, B., Schiehlen, W., Eberhard, P., 2003. Comparison of analytical and experimental results for longitudinal impacts on elastic rods. J. Vib. Control 9 (1–2), 157–174.

Idesman, A., Samajder, H., Aulisa, E., Seshaiyer, P., 2009. Benchmark problems for wave propagation in elastic materials. Comput. Mech. 43 (6), 797–814.

Israelachvili, J.N., 1991. Intermolecular and Surface Forces. Academic Press, London.

Iverson, K.E., 1962. A Programming Language. John Wiley & Sons, New York.

Jayadeep, U.B., Bobji, M.S., Jog, C.S., 2014. Energy loss due to adhesion in longitudinal impact of elastic cylinders. Eur. J. Mech. A/Solids 45, 20–31.

Lapczyk, I., Rajagopal, K.R., Srinivasa, A.R., 1998. Deformation twinning during impact - numerical calculations using a constitutive theory based on multiple natural configurations. Comput. Mech. 21 (1), 20–27.

Ma, C.C., Huang, K.C., 1996. Analytical transient analysis of layered composite medium subjected to dynamic inplane impact loadings. Int. J. Solids Struct. 33 (28), 4223–4238.

Nicholas, T., Recht, R.F., 1990. Introduction to impact phenomena. In: Zukas, J.A. (Ed.), High Velocity Impact Dynamics. Wiley-Interscience, New York, pp. 1–63.

Nonaka, T., Clifton, R.J., Taichirookazaki, T., 1996. Longitudinal elastic waves in columns due to earthquake motion. Int. J. Impact Eng. 18 (7–8), 889–898.

Oberkampf, W.L., Roy, C.J., 2010. Verification and Validation in Scientific Computing. Cambridge University Press, Cambridge.

Randow, C.L., Gazonas, G.A., 2009. Transient stress wave propagation in one-dimensional micropolar bodies. Int. J. Solids Struct. 46, 1218–1228.

Rossikhin, Y.A., Shitikova, M.V., 2007. Analysis of a hyperbolic system modelling the thermoelastic impact of two rods. J. Therm. Stresses 30 (9–10), 943–963.

Scheidler, M., Gazonas, G.A., 2001. Analytical and computational study of one-dimensional impact of graded elastic solids. In: Furnish, M.D., Thadhani, N.N., Horie, Y. (Eds.), Shock Compression of Condensed Matter, AIP 0-7354-0068-7, vol. 23 (1), pp. 689–692.

Schwarz, C., Fischer, F.D., Werner, E., Dirschmid, H.J., 2010. Impact of an elastic rod on a deformable barrier: analytical and numerical investigations on models of a valve and a rod-shaped stamping tool. Arch. Appl. Mech. 80 (1, SI), 3–24.

Shi, P., 1998. The restitution coefficient for a linear elastic rod. Math. Comput. Model. 28 (4–8), 427–435.

Stronge, W.J., 2000. Impact Mechanics. Cambridge University Press, Cambridge, UK.

Sun, J., Xu, X., Lim, C.W., 2013. Localization of dynamic buckling patterns of cylindrical shells under axial impact. Int. J. Mech. Sci. 66, 101–108.

Talebian, S.T., Tahani, M., Abolbashari, M.H., Hosseini, S.M., 2013. Response of multiwall carbon nanotubes to impact loading. Int. J. Mech. Sci. 37 (7), 5359–5370.

Velo, A.P., Gazonas, G.A., Ameya, T., 2009. z-transform methods for the optimal design of one-dimensional layered elastic media. SIAM J. Appl. Math. 70 (3), 762–788.

Wang, Z.P., Sun, C.T., 2002. Modeling micro-inertia in heterogeneous materials under dynamic loading. Wave Motion 36 (4), 473–485.

Werner, E.A., Fischer, F.D., 1995. The stress state in a moving rod suddenly elastically fixed at its trailing end. Acta Mech. 111 (3–4), 171–179.

Wuensche, M., Zhang, Ch., Sladek, J., Sladek, V., Hirose, S., Kuna, M., 2009. Transient dynamic analysis of interface cracks in layered anisotropic solids under impact loading. Int. J. Fract. 157 (1–2), 131–147.

Yu, S.J., Yang, L., Lowe, R.L., Bechtel, S.E., 2010. Numerical simulation of linear and nonlinear waves in hypoelastic solids by the CESE method. Wave Motion 47 (3), 168–182.


[17] These relations can be established independently of (A.6)–(A.9). Jumps in velocity and stress at the back (front) face must agree with jumps across the corresponding forward (backward) propagating transmitted shock in the backing medium (flyer), which are related by (A.10) ((A.11)).

1 (PDF) DEFENSE TECHNICAL INFORMATION CTR DTIC OCA

2 (PDF) DIRECTOR US ARMY RESEARCH LAB RDRL CIO LL IMAL HRA MAIL & RECORDS MGMT

1 (PDF) GOVT PRINTG OFC A MALHOTRA

62 (PDF) DIR USARL
RDRL CIH C
J KNAP
RDRL WM
B FORCH
S KARNA
J MCCAULEY
RDRL WML B
I BATYREV
J BRENNAN
E BYRD
S IZVYEKOV
W MATTSON
B RICE
D TAYLOR
N WEINGARTEN
RDRL WML H
B AYDELOTTE
C MEYER
D SCHEFFLER
B SCHUSTER
RDRL WMM
J BEATTY
R DOWDING
J ZABINSKI
RDRL WMM B
T BOGETTI
C FOUNTZOULAS
C DECKER
G GAZONAS
D HOPKINS
B LOVE
B POWERS
T WALTER
R WILDMAN
C YEN
J YU
RDRL WMM D
A GAYNOR
B MCWILLIAMS
S WALSH
RDRL WMM E
J LASALVIA
RDRL WMM F
M TSCHOPP
RDRL WML G
J ANDZELM
T CHANTAWANSRI
J LENHART
C RINDERSPACHER
T SIRK
Y SLIOZBERG
RDRL WMP
S SCHOENFELD
RDRL WMP B
S SATAPATHY
M SCHEIDLER
A SOKOLOW
T WEERASOORIYA
RDRL WMP C
R BECKER
S BILYK
T BJERKE
D CASEM
J CLAYTON
M GREENFIELD
B LEAVY
J LLOYD
C MEREDITH
S SEGLETES
A TONGE
C WILLIAMS
RDRL WMP D
R DONEY
C RANDOW
S SCHRAML
M ZELLNER

INTENTIONALLY LEFT BLANK.